JOURNAL OF GEOPHYSICAL RESEARCH: ATMOSPHERES, VOL. 118, 4748–4766, doi:10.1002/jgrd.50330, 2013

CALIOP and AERONET aerosol optical depth comparisons: One size fits none

A. H. Omar,[1] D. M. Winker,[1] J. L. Tackett,[1,2] D. M. Giles,[3,4] J. Kar,[1,2] Z. Liu,[1,5] M. A. Vaughan,[1] K. A. Powell,[1] and C. R. Trepte[1]

Received 25 July 2012; revised 11 March 2013; accepted 12 March 2013; published 29 May 2013.

[1] We compare the aerosol optical depths (AOD) retrieved from backscatter measurements of the Cloud-Aerosol Lidar with Orthogonal Polarization (CALIOP) aboard the Cloud Aerosol Lidar Infrared Pathfinder Satellite Observations (CALIPSO) satellite with coincident Aerosol Robotic Network (AERONET) measurements. Overpass coincidence criteria of ±2 h and within a 40 km radius are satisfied at least once at 149 globally distributed AERONET sites from 2006 to 2010. Most data pairs (>80%) use AERONET measurements acquired ±30 min of the overpass. We examine the differences in AOD estimates between CALIOP and AERONET for various aerosol, environmental, and geographic conditions. Results show CALIOP AOD are lower than AERONET AOD especially at low optical depths as measured by AERONET (500 nm AOD < 0.1). Furthermore, the median relative AOD difference between the two measurements is 25% of the AERONET AOD for AOD > 0.1. Differences in AOD between CALIOP and AERONET are possibly due to cloud contamination, scene inhomogeneity, instrument view angle differences, CALIOP retrieval errors, and detection limits. Comparison of daytime to nighttime number of 5 km × 60 m (60 m in the vertical) features detected by CALIOP show that there are 20% more aerosol features at night. We find that CALIPSO and AERONET do not agree on the cloudiness of scenes. Of the scenes that meet the above coincidence criteria, CALIPSO finds clouds in more than 45% of the coincident atmospheric columns AERONET classifies as clear.

Citation: Omar, A. H., D. M. Winker, J. L. Tackett, D. M. Giles, J. Kar, Z. Liu, M. A. Vaughan, K. A. Powell, and C. R. Trepte (2013), CALIOP and AERONET aerosol optical depth comparisons: One size fits none, *J. Geophys. Res. Atmos.*, *118*, 4748–4766, doi:10.1002/jgrd.50330.

1. Introduction

[2] The Cloud-Aerosol Lidar and Infrared Pathfinder Satellite Observations (CALIPSO) mission is a collaboration between NASA and Centre National d'Études Spatiales and was launched in April 2006 to provide vertically resolved measurements of cloud and aerosol distributions [*Winker et al.*, 2007, 2009]. CALIPSO flies in a 705 km Sun-synchronous polar orbit with a 16 day repeat cycle and an equator-crossing time of about 1330 local solar time. The primary instrument on the CALIPSO satellite is the Cloud-Aerosol Lidar with Orthogonal Polarization (CALIOP), a near-nadir viewing two-wavelength polarization-sensitive instrument. CALIOP data are used for profiling cloud and aerosol layers and, to the limit of signal attenuation, determination of cloud thermodynamic phase and aerosol type, and retrievals of aerosol and cloud extinction coefficient profiles.

[3] The unique nature of CALIOP measurements make it quite challenging to validate the attenuated backscatter profiles, aerosol type, and cloud phase, all of which are used to retrieve extinction and optical depth [*Omar et al.*, 2009; *Young and Vaughan*, 2009]. With the exception of a few regions (e.g., Japan and Europe) where this is possible using lidar networks, most of the world is not equipped to make measurements that could be used to directly validate these fundamental products. CALIOP's near-nadir (~3° off nadir) zero swath measurement geometry limits the usefulness of ground sites that are located far from the CALIPSO ground track [cf. *Anderson et al.*, 2003]. The Aerosol Robotic Network (AERONET), with its wide distribution throughout the world, affords a unique data set for intercomparison with CALIOP aerosol optical depths (AOD). The AERONET Sun photometer and CALIOP are both well calibrated with algorithms that are well characterized [*Dubovik and King*, 2000; *Dubovik et al.*, 2002a; *Hu et al.*, 2009; *Liu et al.*, 2009; *Omar et al.*, 2009; *Smirnov et al.*, 2000; *Vaughan et al.*, 2009; *Young and Vaughan*, 2009]. For this study we use AERONET Level 2 quality assured products and CALIPSO 5 km Version 3 provisional products.

[1]NASA Langley Research Center, Hampton, Virginia, USA.
[2]Science Systems and Applications Inc. (SSAI), Hampton, Virginia, USA.
[3]NASA Goddard Space Flight Center, Greenbelt, Maryland, USA.
[4]Sigma Space Corporation, Greenbelt, Maryland, USA.
[5]National Institute of Aerospace, Hampton, Virginia, USA.

Corresponding author: A. H. Omar, NASA Langley Research Center, Science Directorate, MailStop 475, Hampton, VA 23681, USA. (ali.h.omar@nasa.gov)

2169-897X/13/10.1002/jgrd.50330

[4] AERONET AOD comparisons with satellite measurements have been used extensively to estimate satellite measurement uncertainties, improve algorithm development, and data assimilation. Multi-angle Imaging SpectroRadiometer (MISR) and AERONET AOD (τ_a) are generally in agreement with 70% to 75% of MISR AOD within $0.05\tau_a$ [*Kahn et al*., 2005, 2010]. The Moderate Resolution Imaging Spectroradiometer (MODIS) team has conducted extensive validation exercises using AERONET over both land and ocean [*Chu et al*., 2002; *Levy et al*., 2010; *Remer et al*., 2002] and found good agreements (within 2% over the ocean and $0.05 \pm 0.2\tau_a$ over land). A comparison of the POLarization and Directionality of the Earth's Reflectances (POLDER) AOD retrievals to nearly collocated Sun photometer measurements found excellent agreement (regression slope very close to 1) for AOD less than 0.7 [*Goloub et al*., 1999]. *Bréon et al*. [2011] compared several satellite AOD measurements to AERONET and found the most favorable correlations for POLDER and MODIS AOD retrievals. *Kittaka et al*. [2011] found CALIPSO Version 2 AOD and MODIS AOD agreed to within the expected uncertainty of the MODIS over-ocean product. *Kacenelenbogen* [2011] compared MODIS, POLDER, High Spectral Resolution Lidar, AERONET, and CALIOP during one day of the CALIPSO and Twilight Zone validation campaign and found that the CALIOP retrieved AOD was a factor of two lower than the highest values measured. More recently, *Redemann et al*. [2012] compared MODIS AOD with CALIPSO Version 2 and Version 3 AOD and found the CALIOP AOD lower. They suggest several useful screening criteria including cloud cleared columns, retrieval methods, and maximum relative errors. AERONET measurements have also been used for aerosol transport model development and assimilation. To develop a modified product for a near real-time assimilation into a forecasting model, *Zhang and Reid* [2006] used AERONET to filter outliers and noisy records in the MODIS AOD over global oceans.

[5] This paper compares the measurements and provides explanations of some differences between CALIOP AOD at 532 nm and AERONET AOD at 500 nm. While uncertainties in CALIOP calibrations and inversion algorithms are significant, probably more significant than the errors discussed in this paper, these are best tackled by lidar-to-lidar comparisons of backscatter and extinction. AOD comparisons on the other hand help us understand column-scale phenomena such as undetected layers, cloud contamination, and aerosol homogeneity. We assume that the differences due to the spectral variation (500 to 532 nm) between the two instruments are negligible compared to other sources of differences in the AOD. Throughout the paper, we define coincident AERONET/CALIOP data points as those where an AOD has been reported by both instruments within colocation criteria of 40 km radius and ± 2 h. This study uses CALIPSO quality assurance flags for retrieval uncertainty, cloudiness, aerosol layer location, and aerosol homogeneity to screen the data. The CALIOP data used are the profile products with vertical and horizontal resolutions of 60 m and 5 km, respectively. We also examine diurnal differences in the number of aerosol layers CALIOP detects. For quantitative analyses of these differences, we use CALIOP aerosol "features" defined as 5 km $\times$ 60 m (60 m in the vertical) segments of aerosol layers.

[6] In sections 2 and 3, we introduce aspects of CALIOP and AERONET measurements relevant to these studies, and discuss the methodology in section 4. In section 5 we present results of the comparison. Case studies at a number of sites are presented in section 6. We then use screening criteria to repeat the regression for all coincidences in section 7, followed by concluding remarks and recommendations in section 8.

2. CALIPSO Overview

[7] Data used in this study are the CALIOP column AOD in the CALIPSO Level 2 Version 3 aerosol profile products. Dimensions of these products are 5 km (along the CALIPSO ground track) by 60 m in the vertical. CALIOP column AOD are obtained by integrating the aerosol extinction profile. At 532 nm, the lidar calibration coefficient is determined by fitting the range corrected lidar signal between altitudes of 30 and 34 km to a modeled molecular profile [cf. *Powell et al*., 2009; *Young and Vaughan*, 2009]. Molecular backscatter is calculated from profiles of the molecular number density and ozone absorption coefficient obtained from the NASA Global Modeling and Assimilation Office [*Bloom et al*., 2005]. AOD uncertainties, which include the uncertainties in calibration coefficient, extinction to backscatter ratio (S_a) needed for the extinction retrieval, and retrieval errors [*Young et al*., 2012], are reported in the Level 2 CALIOP products. Indicators of the quality of AOD retrievals include the Extinction Quality Control (ExtQC) flag, and the presence of clouds in any part of the 5 km column, herein referred to as cloudiness. CALIPSO Data Quality Summaries and the CALIPSO Users Guide (http://www-calipso.larc.nasa.gov/resources/calipso_users_guide/) are a good resource for a detailed discussion of CALIOP accuracy, uncertainty, and data quality flags.

[8] Retrieval uncertainties propagate through the chain of algorithms used for creating each successive data product thus eventually impacting the accuracy of the column AOD. Errors in the CALIOP AOD arise from inaccurate or incomplete detection and misclassification of aerosol/cloud layers and retrieval errors. Both of these are influenced by signal-to-noise ratios (SNRs), which are lower during daytime when all coincidences with AERONET are found. Additional retrieval errors arise from the use of an incorrect S_a in the inversion of the lidar single scattering equation as a result of the wrong choice of aerosol model. The CALIOP algorithm uses one of six aerosol types: clean continental, clean marine, dust, polluted continental, polluted dust, and smoke with 532 nm (1064 nm) S_a of 35 sr (30 sr), 20 sr (45 sr), 40 sr (55 sr) 70 sr (30 sr), 55 sr (48 sr), and 70 sr (40 sr), respectively [*Omar et al*., 2009]. If the type is incorrectly chosen, the wrong lidar ratio is used in the extinction retrieval leading to errors in the CALIOP AOD. Multiple scattering effects, which are not taken into account in this study, can also be a source of CALIOP AOD error in retrievals of dense dust [*Liu et al*., 2011].

[9] When comparing CALIOP data with AERONET, differences can result if the atmospheric column at the coincident station is not homogenous. We use the root mean square error (RMSE) of the CALIOP 5 km column AOD to estimate of the departure of the AOD of a 5 km column from the mean of 16 adjacent 5 km columns, i.e., the 80 km mean

AOD, corresponding to a 40 km radius centered at the coincidence point.

[10] The CALIOP AOD used in this study is the tropospheric column AOD and does not include stratospheric AOD. Studies of the CALIPSO measurements show that the maximum global mean stratospheric AOD during the period of this study does not exceed 0.008 [*Vernier et al*., 2011] with peak values occurring in July 2007 following the Soufriere Hills and Tavurvur volcanic eruptions in 2006. These values are well below uncertainties in the CALIPSO column AOD and are considered negligible for this study.

2.1. Retrieval Description

[11] CALIPSO algorithms detect features such as cloud and aerosol layers by identifying those regions where the measured data lies significantly above the expected molecular atmospheric backscatter signal. To maximize the detection of weakly scattering layers while still reliably detecting dense layers, the CALIPSO algorithm development team has designed the Selective, Iterated Boundary Location (SIBYL) algorithm, discussed in detail in *Vaughan et al*. [2009]. SIBYL incorporates an adaptive profile scanning engine into a multiresolution averaging scheme of backscatter profiles that identifies successively optically thinner layers using increasingly coarser averaging to enhance SNR. The threshold-based detection scheme used by SIBYL will miss optically thin features that fall below the detection threshold. By the same token, noise excursions can lead to false identification of nonexistent features. These excursions can also elevate the backscatter signal sufficiently to cause the cloud aerosol discrimination (CAD) algorithm [*Liu et al*., 2009] to identify the features as clouds when they are actually aerosols. Because CALIPSO algorithms determine cloud and aerosol optical depths in the same column, the misclassification of aerosol as cloud depresses the column AOD, in some cases quite appreciably by assigning AOD to cloud optical depth. This is discussed in more detail in section 5.3.

[12] Profiles of particle backscatter and extinction coefficients are retrieved by the hybrid extinction retrieval algorithm [*Young and Vaughan*, 2009]. The hybrid extinction retrieval algorithm retrieves the backscatter and extinction using boundaries identified in SIBYL, and in the case of multiple layers, starting with the topmost layer. The downward progression of the classification and retrieval allows correction in the lower layers for attenuation in the upper layers. The retrieval requires S_a that is estimated from the aerosol type classification scheme described in *Omar et al*. [2009].

2.2. Extinction Quality Control Flags

[13] CALIPSO ExtQC flags provide insight into the assumptions invoked during the retrieval of the extinction coefficient from the lidar attenuated backscatter measurements. For unconstrained cases, the particulate S_a (i.e., S_a of the aerosol particles) chosen for a scene is assigned based on an aerosol model [*Omar et al*., 2009]. Extinction retrievals can be constrained by estimating the two-way transmittance and adjusting the particulate S_a iteratively until the retrieved particulate two-way transmittance differs from the supplied constraint by less than some predefined value [*Young*, 1995; *Young and Vaughan*, 2009]. ExtQC values of 0 identify unconstrained retrievals where the initial estimate of lidar ratio remains unchanged during the solution process. ExtQC values of 1 identify constrained retrievals. The rest of the flags (with the exception of ExtQC = 16, which denotes opaque layers) indicate several conditions resulting in changes to the S_a for obtaining an extinction solution.

[14] In CALIPSO data files, ExtQC flags of 0 or 1 denote the AOD estimate with the least uncertainty related to the extinction retrieval. About 5% of the coincident points used for this study have CALIOP AOD with ExtQC values greater than 1. In general, optically thin layers found in the free troposphere may be detected at lower horizontal resolutions (e.g., 80 km instead of 5 km) and may themselves exhibit ExtQC values greater than 1. There is therefore a greater probability of these layers overlying lower layers detected at higher horizontal resolution, say 5 km. These horizontally overlapping and vertically distributed layers introduce uncertainty into the 5 km column AOD, should the upper layers attenuate the signal to such an extent that AOD of the lower layers (and thus the column AOD) becomes relatively uncertain. In extreme cases (e.g., totally attenuating layers), the ExtQC flag provides information that can be used to filter out such columns. Checking at least one 5 km column before and after the coincident point will ease this concern, albeit not in all cases.

[15] Errors due to changes in S_a used to achieve a solution from an otherwise intractable set of conditions are usually large. Therefore, although these cases are few, the errors, especially for cases where S_a is increased (ExtQC = 4), bias comparisons disproportionately. Improper cloud clearing is likely to result into solutions that require a reduction of the assigned S_a (ExtQC = 2) and therefore introduces a high bias. We exclude these cases from the analyses and use CALIOP AOD with ExtQC values of 0 and 1 for the screened data.

3. AERONET Overview

[16] The Aerosol Robotic Network (AERONET) is a federated ground-based instrument network measuring and characterizing aerosol properties including AOD [*Holben et al*. 1998]. The global distribution of Cimel Sun and sky scanning radiometers offers standardized products for regional to global scale aerosol monitoring and validation. The Cimel radiometer has ~1.2° full angle field of view for measuring direct Sun, aureole, and sky radiances. Column AOD is computed from direct Sun measurements made in several spectral bands between 340 and 1640 nm. A sequence of three measurements is taken 30 s apart, creating a triplet of observations per wavelength, approximately every 15 min [*Holben et al*., 1998]. Sky and aureole measurements are performed at 440, 670, 870, and 1020 nm wavelengths. These radiance observations are made through a large range of scattering angles from which size distributions, phase functions, and indices of refraction are retrieved [*Dubovik and King*, 2000; *Dubovik et al*., 2002b; *Holben et al*., 1998, 2006].

[17] For this study we used Level 2.0 quality-assured AERONET data. These measurements have prefield and postfield calibration applied and were cloud cleared and manually inspected. Typical total uncertainty in the AERONET AOD for field instruments is ±0.01 to ±0.02

and is spectrally dependent with the higher errors (±0.02) in the UV spectral range [*Eck et al*., 1999]. AERONET conducts a comprehensive cloud screening procedure involving short time (30 s), and diurnal variations of the AOD at multiple wavelengths (*Smirnov et al*. 2000). Although the algorithm works very well, as demonstrated by *Smirnov et al*. [2000], in some cases, temporal variations in the AOD due to dust may be misidentified as cloud and rejected [*Giles et al*., 2011]. Conversely, some homogeneous cirrus clouds, observed in tropical regions of Southeast Asia [*Chew et al*., 2011; *Huang et al*., 2011] that are relatively uniform and stable can exhibit such small variations in the solar triplet measurement that the scene is classified as cloud free by the AERONET cloud screening algorithms. *Chew et al*. [2011] found that this induces a positive definite bias in the Level 1.5 and 2 AERONET AOD typically exceeding 0.03.

[18] In comparing MODIS and AERONET AOD, *Levy et al*. [2010] noted that the AERONET view is biased toward the clear sky, whereas the MODIS view includes some noncloudy pixels within cloud fields that are physically different from clear sky fields. This bias is expected because the AERONET aerosol retrieval protocol inherently depends on a mainly cloud-free path. For example, the AERONET instrument view angle may be unobstructed although clouds may be in the vicinity of the measurement affecting the MODIS retrieval. Differences in cloud mask algorithms (where AERONET uses a temporal average and MODIS uses a spatial average) can also contribute to the observed discrepancies. However, utilizing higher spatial resolution (3 km) MODIS products partly mitigated this effect [*Giles et al*. 2011].

4. Coincidence Criteria and Frequency

[19] Allowing relatively large spatial differences between CALIOP and AERONET observations compared will generate a larger data set at the expense of loss of representativeness. *Anderson et al*. [2003] show that mesoscale variability is a common feature of lower-tropospheric aerosol light extinction and that autocorrelation (the similarity between observations as a function of the time/space separation) drops below 80% after 40 km for the most conservative case they considered. The autocorrelation at 160 km is only 50%, indicating a significantly different air mass. The temporal interval for an autocorrelation of 80% is about 3 h. We chose a maximum spatial separation of 40 km for two reasons: (1) it maintains an expected autocorrelation of at least 80% and (2) a 40 km radius forms a diameter of 80 km around the AERONET site. Because the CALIPSO horizontal resolutions are 5, 20, and 80 km, this criterion corresponds to the coarsest resolution of the data.

[20] Measurements and retrievals reported in the Level 2 CALIOP aerosol product are quite different from the aforementioned passive measurements. CALIOP is a near-nadir viewing instrument with a small receiver footprint (~100 m) which, in relation to MODIS, MISR, POLDER, and most other passive measurements, is a pencil line or near-zero swath on the surface. As a result, the number of coincidences with ground validation sites is much smaller. Furthermore, if a site is not within the coincidence circle at the point of closest approach in an orbit, the site is unlikely to ever fall in this circle due to the 16 day repeat orbital schedule and small cross-track variability (<20 km). For example, the range of variability (shortest distance between CALIPSO ground track and AERONET site) is about 14 km at Sede Boker, the site with the most coincidences and 11 km at Ilorin, the site with the second most coincidences (Table 1).

Table 1. Number of Coincidences at AERONET Sites With 10 or More Coincidences During the Period 2006–2010

AERONET Site Name	Coincidences	Lat.	Lon.
SEDE_BOKER	35	30.81	34.56
Ilorin	32	8.31	4.28
Karachi	28	24.86	66.98
La_Parguera	28	17.90	–67.35
Abu_Al_Bukhoosh	25	25.45	52.91
FORTH_CRETE	25	35.39	25.56
Fresno	25	36.73	–120.05
Rome_Tor_Vergata	25	41.86	12.76
Sevastopol	24	44.60	33.45
Dhadnah	22	25.45	56.00
IMS-METU-ERDEMLI	21	36.61	34.49
Arica	17	–18.46	–70.26
Hong_Kong_PolyU	17	22.26	113.96
Lake_Argyle	17	–16.15	128.54
XiangHe	16	39.76	116.96
Munich_University	15	48.22	12.00
Chen-Kung_Univ	14	22.95	119.97
Dakar	14	14.38	–16.88
Mukdahan	14	16.56	104.45
Kanpur	13	26.55	80.45
Monterey	13	36.64	–121.58
Pantnagar	13	29.09	79.81
Key_Biscayne	12	25.76	–80.01
Shirahama	12	33.77	135.72
Skukuza	12	–24.97	31.70
Darwin	11	–12.44	130.79
Mongu	11	–15.23	23.24
Moscow_MSU_MO	11	55.76	37.90
Oostende	11	51.25	3.02
Rio_Branco	11	–9.90	–67.54
Santa_Cruz_Tenerife	11	28.54	–15.87
Tudor_Hill	11	32.30	–64.72
Wallops	11	37.92	–75.61
Dhabi	10	24.54	54.66
EPA-NCU	10	24.94	121.02
IER_Cinzana	10	13.25	–6.06
Paris	10	48.90	2.50

[21] In the four years (2006–2010) covered by this study, over 22,635 instances of CALIPSO overpasses occurred within 40 km of currently active or inactive AERONET sites on the globe. Of these collocations, only a few sites had temporally coincident measurements. Due to reduced sensitivity and/or clouds, CALIOP has no AOD retrieval in about 10% of the overpasses with an AERONET AOD. CALIPSO's orbital configuration provides more frequent overpasses near the poles than in the tropics. However, many of the CALIOP orbit tracks in Polar Regions correspond to conditions where optically thin aerosol layers are presumably undetectable by CALIOP. During polar winters the low Sun angle and short daylight duration reduce the volume of AERONET Level 2.0 AOD measurements. The final tally for all worldwide AERONET sites from 2006 to 2010 is 1081 coincidences representing slightly below 5% of total instances of potential coincident measurements. Thus, we anticipate that this record will grow at about 250 coincidences per year throughout CALIPSO's life if AERONET maintains the current level of operations. Although we used a 2 h temporal

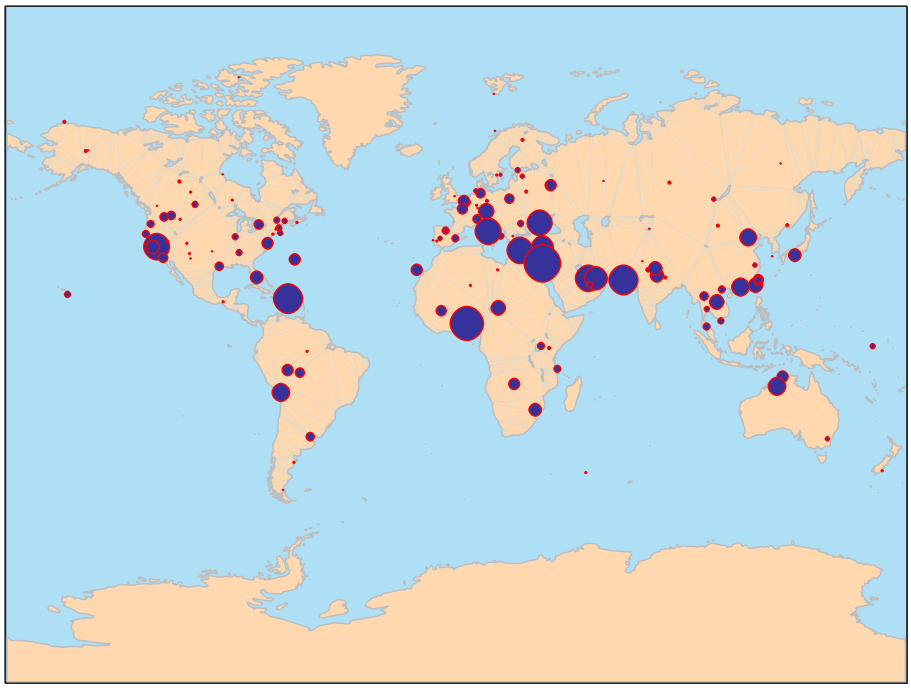

Figure 1. Locations and frequency of the 1081 coincident points at 149 AERONET sites. The diameter of the blue circles is proportional to the number of coincident points. The red dots are sites with less than five coincidences.

coincidence criterion, approximately 80% of coincidences occurred when AERONET AOD measurements were acquired within 30 min of the CALIPSO overpass.

[22] Figure 1 is a map showing all 149 coincident sites in blue circles with red borders. The diameter of the blue circle is directly proportional to the number of coincident points obtained at the site. Sites with few coincidences (less than 5) appear as red dots. The sites with the largest number of coincident measurements were located in the subtropical region (i.e., Sede Boker, Karachi, Fresno, and Abu Al Bukhoosh) and tropics (i.e., Ilorin and La Parguera) (Table 1). Generally, these sites experience significant periods of cloud-free conditions and usable data from both instruments. For sites that have one possible coincidence every 16 days, there are 92 possible overpasses in a 4 year period. Sede Boker and Ilorin generate usable coincidences at rates of 40% and 35%, respectively.

5. Results

5.1. Day/Night Comparisons

[23] Unlike most passive instruments that retrieve AOD from measurements of scattered sunlight, CALIOP has its own source of light and is thus capable of making measurements both at daytime and nighttime. In fact, because sunlight during daytime contributes to signal noise in CALIOP measurements, nighttime measurements exhibit a significantly higher fidelity. The effectiveness of the CALIPSO layer detection scheme is adversely affected by the solar background noise that contaminates the daytime signals. A study of CALIOP day/night performance shows remarkable consistency between the two when compared with a global aerosol visibility analysis model that assimilates MODIS and MISR [*Campbell et al.*, 2012].

[24] Figure 2 shows the frequency distribution of 5 km × 60 m (length × height) aerosol features sorted by mean normalized extinction defined as the optical depth per unit height of the aerosol-containing column. Negative extinctions are a result of negative lidar backscatter measurements and are included for completeness. Significantly more

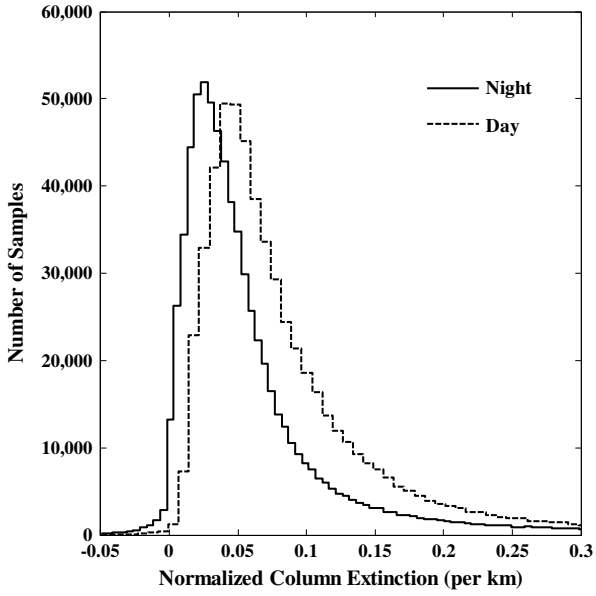

Figure 2. Frequency distributions of the normalized extinction retrieved from CALIOP measurements at daytime and nighttime during August 2006. The normalized extinction is the column AOD normalized by the total height of the aerosol laden column.

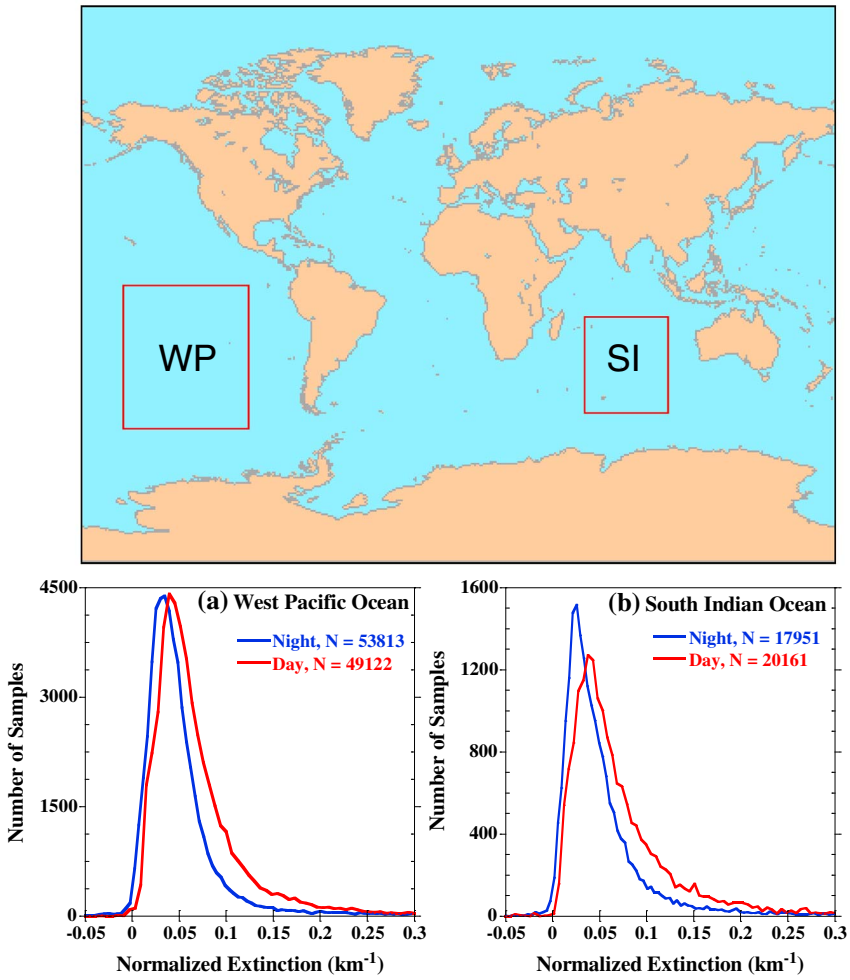

Figure 3. Distributions of day and night aerosol normalized extinction retrievals from CALIOP measurements in two regions (red boxes in the top panel) in the (a) West Pacific (WP) and (b) South Indian (SI) oceans, for August 2007.

aerosol layers were observed at night than during the day for very low extinction (< 0.05). For AOD > 0.05 there are more features at daytime. The enhanced SNR at night means CALIOP is more likely to detect clear sky gaps and hence more layers with smaller AOD at night. At daytime, these layers are not detected as individual layers but rather as aggregates of layers and this may contribute to the higher frequency of larger AOD at daytime.

[25] While the data shown in Figure 2 are global, the same behavior, albeit less pronounced, is observed for relatively pristine deep ocean domains with low mean AOD (regions WP and SI in Figure 3). Considering the remote location of these regions, nominally there should be very small diurnal differences in AOD. There are fewer features of low optical depth at daytime due to the failure to detect very tenuous layers because of diminished signal-to-noise ratios. Additionally, the enhanced SNR and increased sensitivity to clear sky gaps at night could have an effect on the number of features detected [cf. *Campbell et al.*, 2008].

[26] There are about 9% and 11% more features at night (compared to day) in the West Pacific and South Indian oceans, respectively. The modes of both distributions favor lower AOD at night, an indication that more optically thin features are detected at night. The mean values and number of features for each case are shown in Table 2.

[27] Microphysical processes such as humidity growth, nucleation, gas to particle conversion favored by lower nocturnal temperatures [*Seinfeld and Pandis*, 1998] could increase aerosol loading at night. On the other hand, daytime photooxidation reactions of gaseous species such as SO_2

Table 2. Statistics of the Distributions of the Day and Night Normalized Extinction and Number of Features Shown in Figure 2 (Global) and Figure 3 (WP, Western Pacific and SI, South Indian Oceans). Features are Defined as 5 km × 60 m (Length × Height) Areas Containing an Aerosol Layer. [Night-Day]% is the Percent Difference in the Number of Features Observed by CALIOP at Nighttime and Daytime

	Features	Mean (km^{-1})	Median (km^{-1})	[Night-Day]%
Night (Global)	728635	0.07	0.04	+20%
Day (Global)	581144	0.10	0.06	
Night (WP)	53813	0.06	0.04	+9%
Day (WP)	49122	0.07	0.06	
Night (SI)	20161	0.06	0.04	+11%
Day (SI)	17951	0.08	0.05	

[*Hatakeyama et al*., 1985; *Sidebottom et al*., 1972] from dimethyl sulfide lead to more daytime aerosols and thus an enhanced daytime AOD. Furthermore, because AOD depends on wind speed at these remote ocean locations [e.g., *Smirnov et al*., 2003], diurnal wind speed differences may lead to differences in the total AOD. However, differences in the number of optically thin layers between day and night observed by CALIOP are mostly due to challenges associated with layer detection at daytime by the lidar because these are confined to regions of low AOD < 0.05.

[28] CALIOP observes more than 20% fewer aerosol features at daytime than nighttime globally and about 10% fewer daytime features over open oceans where there is reasonable expectation that the day and night number of features should be the same (Table 2). Because CALIOP SNR are best at nighttime, CALIPSO's AOD validation would benefit from a dedicated nighttime field campaign. The U. S. Navy Aerosol Analysis and Prediction System [*Campbell et al*. 2012] evaluated CALIOP nighttime AOD using two-dimensional variational assimilation of MODIS and MISR AOD and found comparable correlations at both daytime and nighttime. A few dedicated (i.e., nonopportunistic) comparisons with AERONET such as the CALIPSO and Twilight Zone [*McPherson et al*., 2010] in the Baltimore/Washington, DC, region during the summer of 2007, and TIGERZ [*Giles et al*., 2011] have been conducted. Both of these were daytime measurements and do not address the undetected optical depth due to poor daytime SNR. CALIOP's near-zero swath and near-nadir pointing measurements are a challenge for opportunistic validation where there is no prior planning or coordination of ground site locations, and the comparisons are post-priori using criteria that are a compromise between data volume and similar air mass. Obtaining nighttime comparisons is therefore critical for establishing the fidelity of CALIPSO retrievals of AOD.

5.2. AERONET-CALIOP AOD Patterns

[29] In Figure 4, we present a time series of the AOD at the two sites with the highest frequency of usable coincidences (i.e., Sede Boker and Ilorin). Sede Boker is a site in the Negev Desert of Israel and experiences predominantly dust and some urban aerosol [*Derimian et al*., 2008]. Ilorin experiences mainly dust and episodic biomass burning smoke [*Eck et al*., 2010]. Error bars are shown for both samples. Missing CALIPSO error bars denote cases where retrievals could not determine an uncertainty. Because of CALIPSO's limited swath and repeat cycle of 16 days, it is possible but unlikely to get two coincidences per month at a site.

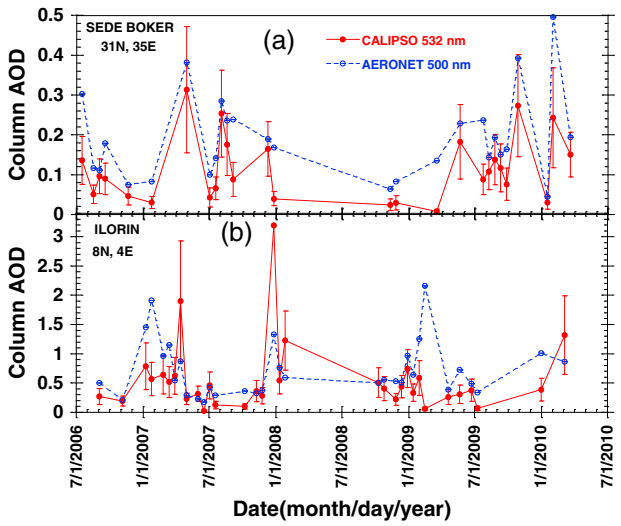

Figure 4. Temporal variation of the AERONET-CALIOP coincident AOD at the two stations with the most coincidences between 2006 and 2010: (a) Sede Boker and (b) Ilorin.

[30] There were very few coincidences for either site from January 2008 to January 2009. The Ilorin site was not in operation for a part (late February to mid-May 2008) of this period. Both instruments show AOD maxima in January at Ilorin corresponding to the peak of the west African biomass burning season. At Sede Boker, both instruments show an AOD that does not vary with season. The four years of data, presented in Figure 4, show a number of gaps and several time periods where good agreement is found (i.e., absolute relative difference less than 40% of the AERONET AOD) at Sede Boker (RMSE = 0.22). The agreement at Ilorin is poorer (RMSE = 0.62). Sede Boker is considerably more cloud-free (79%) compared to Ilorin (34%), and experiences airmasses from desert dust source regions predominantly. Ilorin experiences air masses of Sahara dust and biomass burning in the dry season (January through March) leading to relatively higher AODs in these months. During the wet months (June through September), fine dust is the major constituent [*Nwofor et al*., 2007], associated with lower AOD.

[31] Figures 5 and 6 show comparisons of unscreened (Figures 5a and 6a) clear sky and (Figures 5b and 6b) all sky coincidences during the four years of this data set for both the green (532 and 500 nm) and red (1064 and 1020 nm) channels. Cloudiness is determined using CALIPSO's CAD algorithm. Error bars in the figure (and all subsequent figures) reflect CALIOP calibration and retrieval uncertainties in the reported column AOD in the vertical axis, and a constant value of 0.02 representative of AERONET AOD uncertainty in the horizontal axis [*Eck et al*., 1999; *Holben et al*., 1998; *Smirnov et al*., 2000] with the presumption of no cloud contamination.

[32] Better agreement is apparent for the infrared channel (CALIOP 1064 nm and AERONET 1020 nm) in Figure 5 when compared to the green channel (CALIOP 532 nm and AERONET 500 nm) in Figure 6. The slopes for the green channel are 0.57 and 0.45, for the clear and all sky fits, respectively, compared to 0.91 and 0.82 for the infrared channel. The results are unexpected in light of the higher confidence in the calibration [*Winker et al*., 2009] and S_a [*Omar et al*., 2009] of CALIOP at 532 nm. There were 600 clear sky cases out of 1081 coincidences (Table 3) in this 4 year data set. Most of the coincident AOD are less than 1. Records with AOD >1 are not shown in the figures for clarity. At daytime the largest contribution to the 532 nm noise is due to the solar background while the 1064 nm signal noise is always dominated by diurnally independent detector dark noise.

[33] An analysis of the correlations between cloud-cleared CALIOP 532 nm and AERONET 500 nm AOD at the 149 land and coastal/oceanic sites showed that the differences between the CALIOP AOD retrievals and the AERONET AOD measurements are independent of the surface type for this data set (2006–2010). There were 468 coastal/oceanic

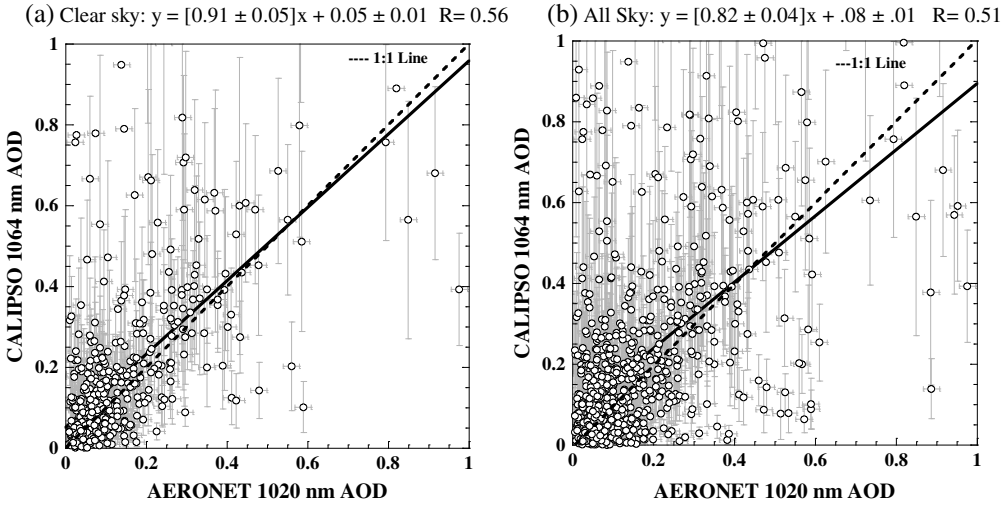

Figure 5. (a) Clear sky and (b) all sky infrared channel (1064 nm CALIPSO and 1020 nm AERONET) AOD regression and linear fits. The black line is the linear fit described by the regression equation coefficients (± standard errors). The dashed line is the 1:1 line. Gray error bars denote CALIOP AOD uncertainty, and a fixed AERONET AOD uncertainty estimate (0.02).

data points at 57 sites and 613 land data points at 92 sites (Figure 7). Not only are the two regressions shown in Figure 8 very similar, they also closely match the regressions of the whole data set presented in Figure 6. CALIPSO applies the same algorithm to the land and ocean surfaces if the aerosol type is the same, e.g., dust AOD over the ocean is retrieved with exactly the same algorithms as dust AOD over land. The similarities in the regressions are thus expected.

[34] *Campbell et al*. [2012] compared 2007 CALIOP nighttime AOD in 1° × 1° bins with an aerosol forecast model equipped with a two-dimensional assimilation scheme for AOD data sets from Terra and Aqua MODIS and MISR. They found differences in the offsets between land and ocean. In particular, CALIOP AOD are higher over land and nearly equal over water. These differences reflect comparisons between CALIOP and different instruments using different screening and quality assurance criteria. In particular, MODIS AOD retrieval algorithms and accuracies over land and water are quite different and may explain why *Kittaka et al*. [2011] also found larger differences between CALIOP and MODIS over land than water. Comparing MODIS AOD to CALIOP AOD, *Redemann* [2012] found broader distributions in the AOD difference over land than water and attributed these uncertainties in the MODIS over-land retrievals and differences in CALIOP aerosol type. On the other hand, the accuracy and variability of the AERONET AOD used in this study are not as sensitive to surface type.

[35] *Bréon et al*. [2011] compared MODIS, MISR, and POLDER AOD with AERONET using criteria developed for MODIS AOD retrievals [*Remer et al*., 2005] shown in equation (1), where the error $\Delta\tau$, is defined by,

$$\Delta\tau = 0.03 + 0.05\tau_{AER} \text{ over ocean, and} \quad (1a)$$

$$\Delta\tau = 0.05 + 0.15\tau_{AER} \text{ over land.} \quad (1b)$$

where τ_{AER} is the AERONET optical depth.

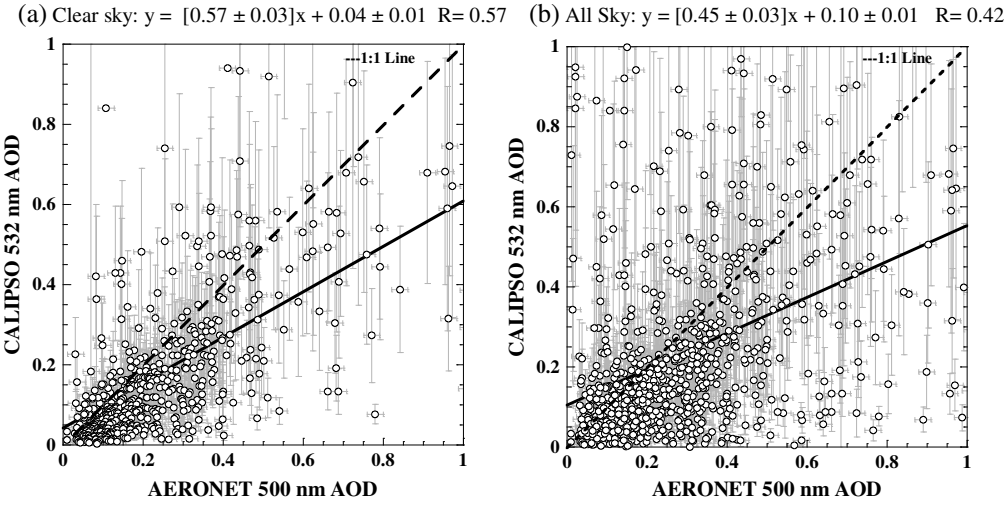

Figure 6. (a) Clear sky and (b) all sky green channel (532 nm CALIPSO and 500 nm AERONET) AOD regression, as described in the caption of Figure 5.

Table 3. Percentage of CALIOP Retrievals Falling Within the Expected Error as Defined in Equation (2), Equation (1a) (Over Ocean), and Equation (1b) (Over Land)

	Equation (2)		Over Land		Over Ocean		Number of Samples
	1064 nm	532 nm	1064 nm	532 nm	1064 nm	532 nm	
All	73.8	56.5	61.1	39.7	41.0	21.7	1081
Clear Sky	81.0	62.7	70.0	47.7	51.2	25.8	600

[36] From *Winker et al*. [2009], the expected error for CALIOP is

$$\Delta\tau = 0.05 + 0.40\tau \quad (2)$$

over both land and ocean.

[37] *Bréon et al*. [2011] calculated an Ångström exponent based on the 532 and 1064 nm AOD and used it to interpolate CALIOP AOD to wavelengths of 670 nm, 870 nm, and extrapolate to 500 nm. Using a coincidence criterion of 150 km and 30 min they found that 23.5%, 31.7%, and 32.9% of AOD at 500, 670, and 870 nm, respectively, fell within the MODIS over-ocean expected errors (equation (1a)). For comparison, 40–60% of MODIS and POLDER AOD were within the MODIS expected error over the ocean and 60–80% over land. Table 3 shows the fraction of CALIOP AOD falling within the expected error for CALIOP retrievals (equation (2)) and falling within the MODIS expected error (equation (1)) for all sky and clear sky. In all cases, there is a significant improvement in the fraction of good measurements for clear sky compared to all sky. These begin to approach the accuracies of the larger swath measurements of POLDER and MODIS for over land cases at 1064 nm.

[38] For the sake of brevity we confine the remainder of this paper to the 532 nm CALIOP AOD comparisons (Figure 6). Further analysis of the infrared retrievals is planned following pending updates and improvements in the 1064 nm calibration [*Vaughan et al*., 2012], which will lead to more accurate retrievals and thus a more meaningful comparison with AERONET 1020 nm AOD. In the following sections, we explore several reasons why CALIOP AOD is lower than AERONET in the regressions of Figure 6.

5.3. Effect of Cloud Fraction on the AERONET-CALIOP Intercomparison

[39] Aerosol optical depth measurements by passive methods (MODIS, AERONET, etc.) are susceptible to cirrus contamination [*de Meij et al*., 2007; *Kaufman et al*., 2005, 2006]. *Chew et al*. [2011] found a range in AERONET AOD bias due to unscreened cloud presence of 0.031 to 0.060 over a one year period in Singapore. *Huang et al*. [2011] found a non-negligible percentage of AERONET aerosol data have cirrus contamination (near 25% for measurements at Phimai in South East Asia) when compared with CALIOP and a ground based micro-pulse lidar. Such contamination has the effect of increasing the AERONET AOD and contributes to a high bias mainly in tropical regions where homogeneous thin cirrus clouds are found. If AERONET AOD is available when CALIPSO identifies a significant fraction of clouds in the scene, the CALIOP AOD will be less than the AERONET AOD because a fraction of the CALIOP features do not contribute to the AOD. Whenever AERONET reports a Level 2.0 quality assured AOD, it implies no clouds in the field of view of the

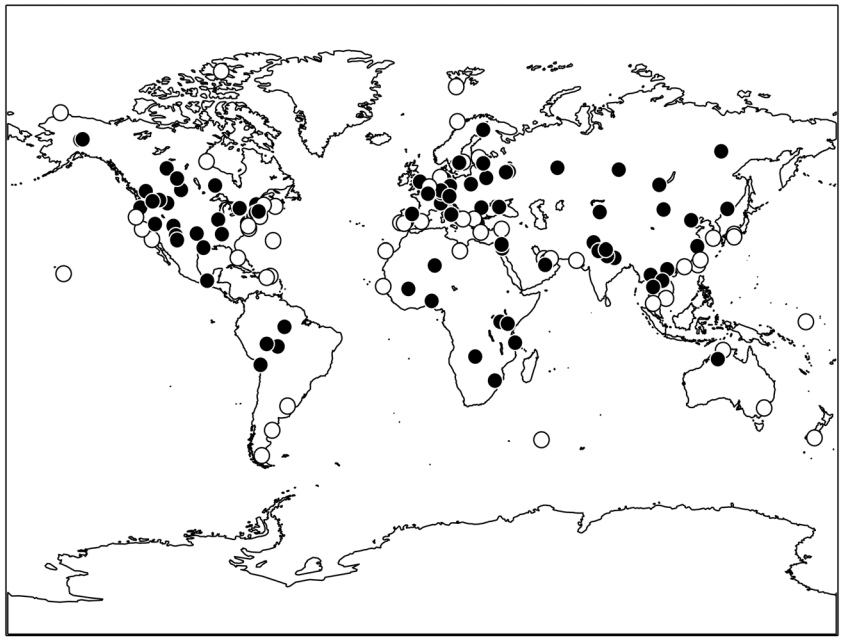

Figure 7. AERONET coastal/oceanic sites (open circles) and land sites (filled circles) at which there were coincidences with the CALIOP AOD retrievals between 2006 and 2010.

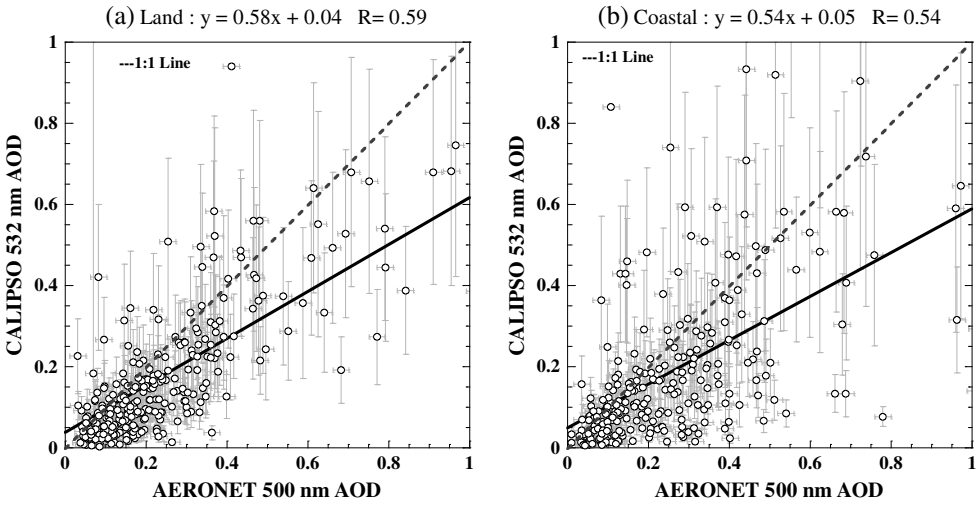

Figure 8. 532 nm CALIOP and 500 nm AERONET AOD regressions at the AERONET land sites and (b) coastal sites. The lines and symbols are as described in the caption of Figure 7.

instrument. However, the overall sky condition may also include a few scattered clouds. In many cases there is an AERONET AOD measurement at a coincidence point at which CALIOP detects clouds. Such cases mean that the atmospheric columns observed by the two instruments are different partly due to temporal, spatial and viewing geometry offsets. These could also be due to differences in the cloud screening methods. Such disagreements are quite frequent for the 2 h and 40 km coincidence criteria used in this study. More than 45% of all coincidences are classified as cloud free by the AERONET cloud screening algorithm and cloudy by the CALIPSO algorithm.

[40] Figure 9a shows the frequency distributions of the CALIOP and AERONET column AOD. Two regions ($0.2 < AOD < 0.5$, and $AOD < 0.1$) within the frequency distributions of the two measurements show a significant difference.

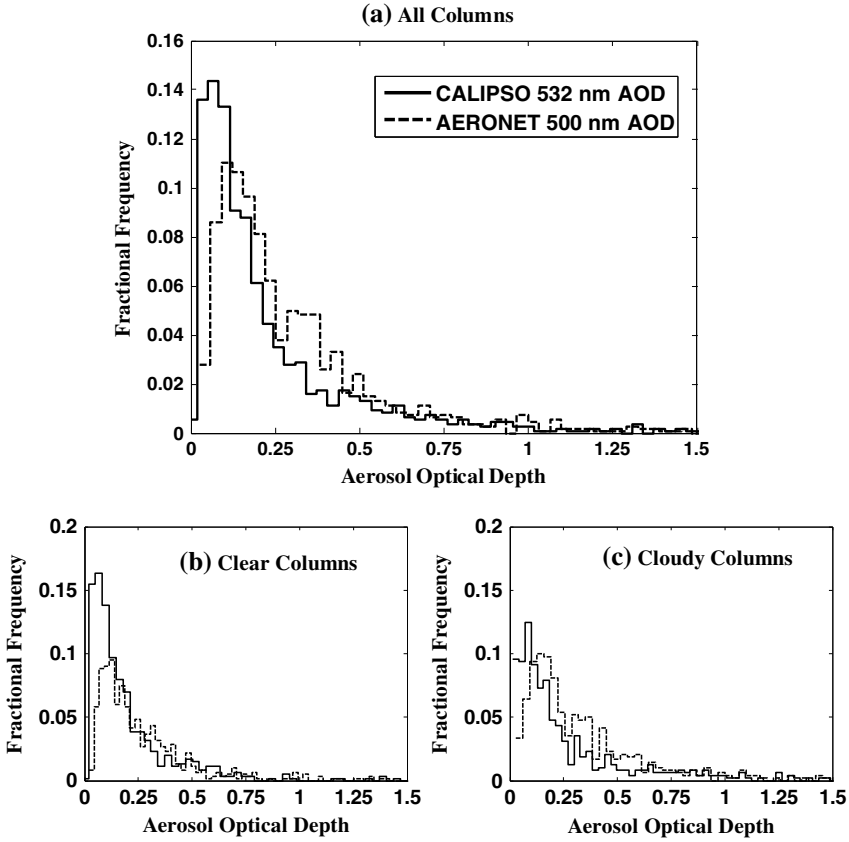

Figure 9. Frequency distributions of the CALIPSO and AERONET AOD of (a) all coincidences, (b) coincidences with a CALIPSO clear columns, and (c) coincidences with CALIPSO cloudy columns.

Table 4. AERONET and CALIOP Green Channel AOD at the Coincidence Points

	CALIOP 532 nm AOD	AERONET 500 nm AOD
Mean	0.237	0.297
Median	0.128	0.200
Standard Deviation	0.325	0.304
Minimum	−0.030	0.009
Maximum	3.192	3.254
Count	1081	1081

In the first region between 0.2 and 0.5, AERONET AOD frequencies are consistently higher. CALIOP AOD may be affected by the misclassification of aerosol layers in the column as clouds, which do not contribute to the AOD. The frequency gap in this region is partly due to differences between the two instruments' detection of cloudy conditions as shown by examining Figures 9b and 9c. In the distribution of the cloudy cases (Figure 9b), the difference in the two distributions in the $0.2 < \text{AOD} < 0.5$ region is larger. In the region ($\text{AOD} < 0.1$), there is a higher frequency of CALIOP AOD in both cases. Table 4 shows the descriptive statistics of the two measurements for all sky cases. While the means are close, the CALIOP median is significantly smaller than the AERONET median.

[41] CALIOP and AERONET coincidences are always separated by some distance. Given the mean separation of 20 km and coincidence criteria discussed in section 4, we investigate the impact of the two instruments encountering different cloud cover conditions. Figure 10 depicts a case where the cloud clearing schemes of the two measurements show very different results. Figure 10a features the CALIOP

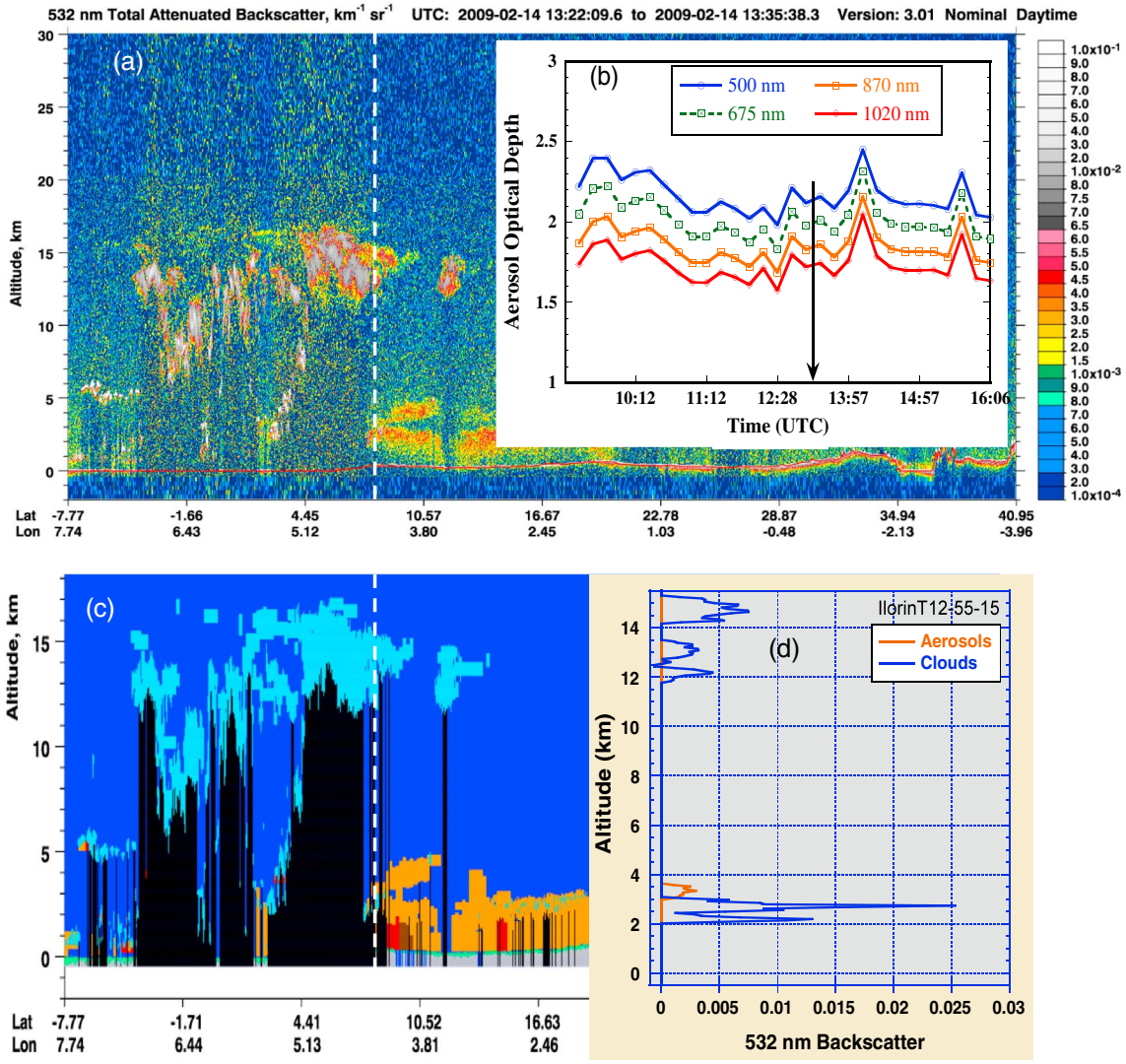

Figure 10. The scene near the Ilorin AERONET station on 14 February 2009 showing (a) CALIOP 532 nm total attenuated backscatter image and (b) the corresponding AERONET AOD variation at several wavelengths near the CALIPSO over flight over Ilorin; (c) the CALIPSO vertical feature mask, with clouds shown in blue and aerosols in orange and uncertain features in red; and (d) the CALIOP cloud and aerosol backscatter profile of the coincident column showing three cloud layers and one aerosol layer. The white dashed lines in Figures 10a and 10c show the coincidence location and the arrow in Figure 10b shows the coincidence time.

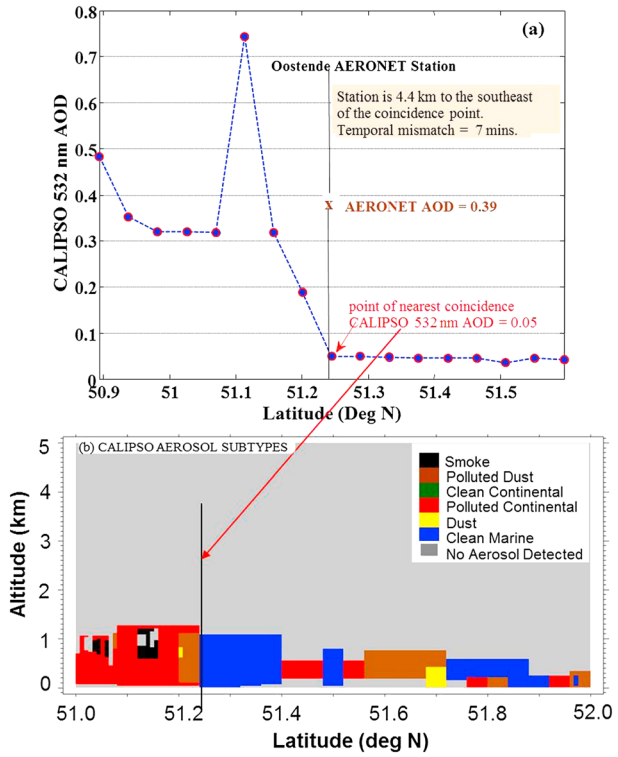

Figure 11. (a) CALIPSO AOD variability compared to the AERONET measurement near the Oostende station and (b) the CALIPSO aerosol subtypes near the station. The vertical line in both plots denotes the coincidence latitude.

532 nm total attenuated backscatter depicting considerable cloudiness near the coincident point (denoted by the white dotted line). The CALIOP retrieval and AERONET measurements of AOD, of 0.06 and 2.16, respectively, were made at the Ilorin site on 14 February 2009 within 5.4 km and 1.5 min of one another. However, while CALIOP depicts an extensive layer of high clouds in the vicinity of the measurements, AERONET did not detect any cloud.

[42] The CALIPSO 5 km columns on both sides of the column of closest coincidence were both cloudy with lowest cloud altitudes of 2.4, 2.1, and 2.4 km for the three adjacent columns centered at the coincidence column. This low altitude opaque cloud blocked CALIPSO's view of most of the aerosol causing an underestimate of AOD. Figure 10c shows the cloud aerosol vertical feature mask for CALIPSO. Layers classified as clouds are blue and those as aerosols are orange. Red and brown indicate layers with unreliable cloud-aerosol classifications. Note also the high fraction of clouds at 10 to 15 km in the vicinity of the measurements. The AERONET Level 2.0 AOD shown in Figure 10b indicates likely cloud-free conditions between the instrument and Sun. The AOD temporal plot shown in Figure 10b shows nearly continuous measurements made between 900 and 1600 UTC. AERONET made continuous measurements hours before and after the coincidence time of 13:25 UTC while CALIPSO recorded considerable cloudiness at or near the same time, including an apparently persistent and spatially extended cirrus cloud deck near 15 km. Figure 10d shows cloud and aerosol backscatter profiles from the CALIPSO Version 3 Level 2 profile product for the coincidence column.

[43] Note that three layers of clouds and one layer of aerosol above the lowest layer of clouds were identified in the coincidence column. Although this measurement fits the coincidence criteria, it is not a valid measurement for comparison and is a good example where screening by the CALIPSO CAD should be used to obtain a valid comparison with AERONET. For the profile shown, the CALIOP Cloud Optical Depth is 0.4. In this case, the contribution of the cirrus Cloud Optical Depth measured by CALIOP is 0.13, approximately 6% of the measured AERONET AOD and not enough to account for the discrepancy between the two instruments. For the measurement in Figure 10b, the Sun photometer pointed at a solar zenith angle of 31° while CALIOP made a near-nadir measurement. Depending on how homogenous the scene near Ilorin was at the time the measurements were made, it is possible that the two instruments viewed different airmasses. The complexity of the scene suggests that there are other considerations such as overhead attenuation. In summary, such scenes are poor candidates for an intercomparison study.

5.4. Aerosol Optical Depths Homogeneity

[44] CALIPSO algorithms retrieved an AOD of 0.05 at the Oostende AERONET station. The temporal and spatial coincidence was 7.5 min and 4.4 km. AERONET measured an AOD of 0.39 at 500 nm. The three consecutive CALIOP 5 km column AOD retrievals observed to the south of the coincidence point have an average AOD of 0.41 (Figure 11). AOD drops off quite rapidly to the north of the station as the spacecraft flies over the North Sea and, conspicuously, the predominant CALIPSO aerosol type switches from polluted continental to clean marine. The AERONET instrument is on the roof of a building in Oostende, Belgium, a

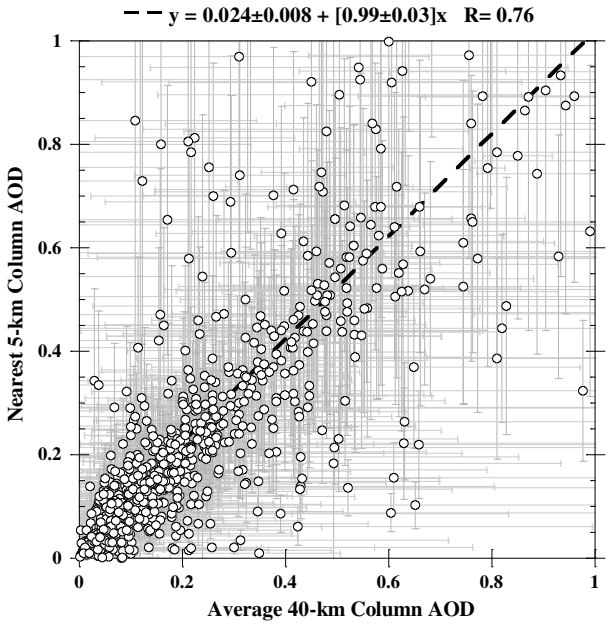

Figure 12. Nearest 5 km column AOD compared to the average 40 km column AOD retrieved from CALIOP. The errors bars in the *y* axis are the 532 nm 5 km column AOD uncertainties reported in the CALIPSO products and the *x* axis error bars are the root mean square error (RMSE) of eight 5 km AOD in a 40 km column.

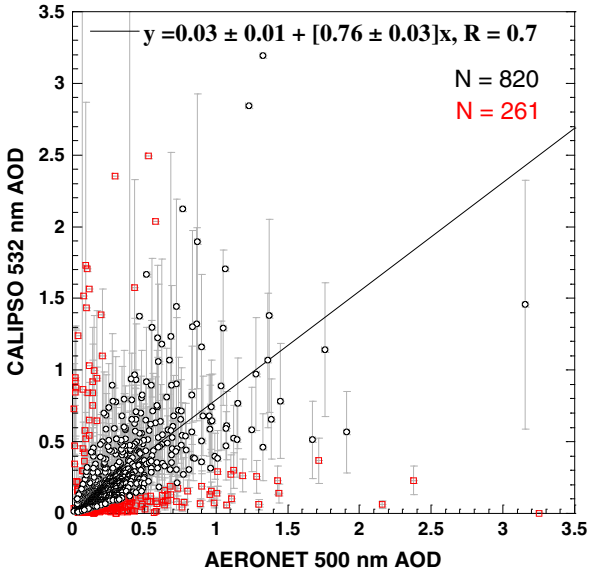

Figure 13. AERONET and CALIOP AOD correlations showing the poorly correlated measurements in red. The vertical bars denote uncertainties in the CALIPSO measurements whenever these are reported.

port city on the coast of the North Sea. Oostende, a transportation hub and resort town is the largest population center on the Belgian coast. The predominant aerosol type on land is urban (polluted continental) and depending on transport, significant pollution outflows are possible.

[45] This scene presents several challenges: (1) These are relatively weak layers and CALIOP did not discern them at 5 km resolution requiring further averaging to increase SNR. They were found (detected) at 20 km averaging. Because AOD is retrieved from 20 km averages here, local variations in aerosol loading especially in going from land to ocean are smoothed out, and (2) the CALIPSO aerosol subtyping scheme favors clean marine types for spherical particles found over the ocean. In this case, the CALIOP subtype of clean marine and the subsequent retrieval of AOD using the smaller (relative to polluted continental) clean marine S_a may have contributed to an underestimate of the CALIOP AOD. In fact for the case illustrated in Figure 11a, all of the 5 km columns to the left of the coincident point have at least one polluted continental layer ($S_a = 70$ sr) and the first four 5 km columns to the right of the coincident point have a single clean marine layer ($S_a = 20$ sr).

[46] Root mean square error for the 5 km CALIOP columns for the case in Figure 11 is 0.25. While the example is somewhat unusual, the frequency of occurrence of similar inhomogeneous scenes is not negligible. The use of RMSE threshold, calculated from the sixteen 5 km segments within a 40 km radius of the coincidence point, to screen out such scenes improves the relevance of the comparisons. For this data set (2006–2010), the effect of using the nearest 5 km column instead of averaging the CALIOP AOD in 40 km columns (i.e., using eight 5 km AOD) is shown in Figure 12. The higher resolution underestimates the average by 0.024. Though the two AOD are related by a slope of nearly 1, the spread in the data shows that there is a significant number of stations at which the nearest 5 km column AOD is different from the 40 km column average.

5.5. Analyses of the Coincidences With Poor Agreement

[47] To analyze the lack of correlation at some coincident points, we examined in particular, the relative magnitudes of the comparative AOD, and the corresponding CALIPSO cloud mask. We found 261 (or 24%) points which are in relatively poor agreement with the AERONET AOD, defined as having an absolute relative error, $|\Delta|\tau$ defined by

$$|\Delta|\tau = \left|\frac{\tau_c - \tau_a}{(\tau_c + \tau_a)/2}\right|, \tag{3}$$

greater than 1.1. In equation (3), τ_c is the CALIOP 532 nm AOD and τ_a is the AERONET 500 nm AOD. In general, the latitudinal distribution of $|\Delta|\tau$ found no relationship between poorly correlated sites and latitude.

[48] Poorly correlated points denoted by the red squares, are shown in Figure 13. The rest of the points, shown as black circles, have an AOD intercept of 0.03 and a regression slope of 0.76.

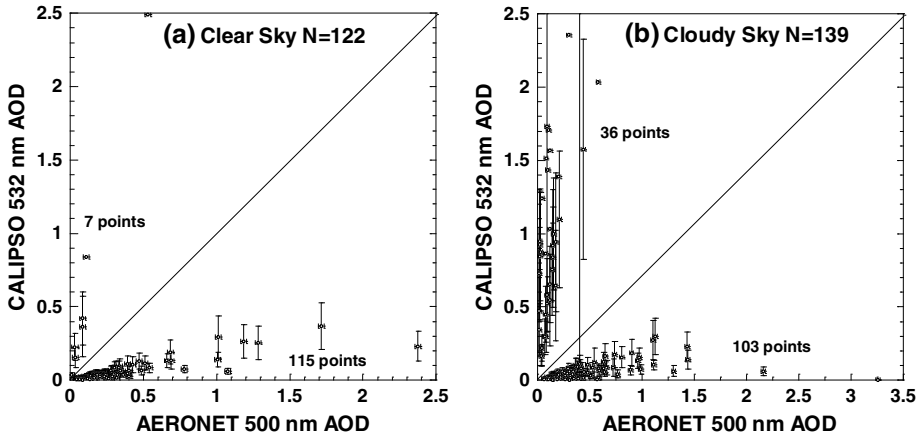

Figure 14. The distributions of points for the poorly correlated sites divided into regions where the CALIOP AOD is greater, and less than the AERONET AOD for the CALIOP-determined (a) clear sky and (b) cloudy sky cases.

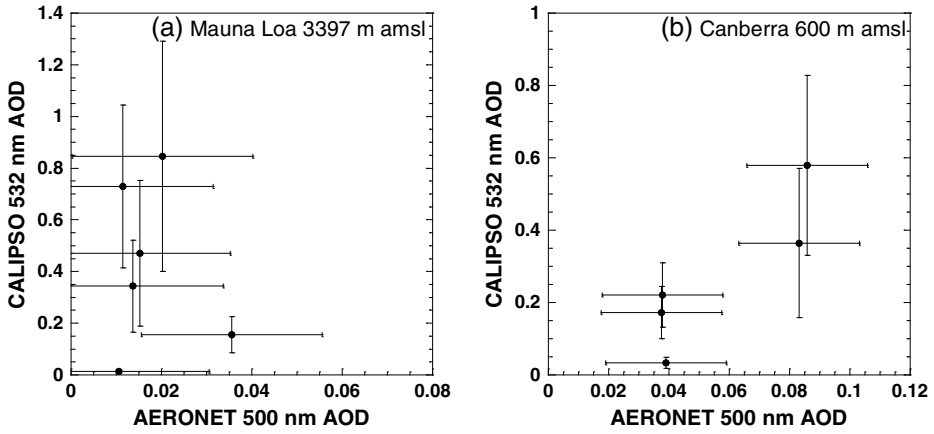

Figure 15. Comparison of AERONET and CALIOP AOD at Mauna Loa (19°N,155°W), and Canberra (35°S, 149°E), for all coincidences between 2006 and 2010. Note that the *x* and *y* axes have different limits.

[49] Points that have an unquantified CALIPSO uncertainty (no gray bars) are ones in which the uncertainty is too large or cannot be estimated such as the case when the ExtQC > 1. Differences in the poorly correlated data set cannot thus be explained by inversion and calibration errors only.

[50] Figure 14 shows regressions of CALIOP-determined (Figure 14a) clear sky and (Figure 14b) cloudy sky cases for the poorly correlated coincidences. In the plots we divided the points into two regions: one with CALIOP AOD greater than AERONET AOD and another with AERONET AOD greater than CALIOP AOD. This partitioning is based on the idea described previously that for normal lidar retrievals, AERONET AOD > CALIOP AOD. Cases of AERONET AOD > CALIOP AOD occur with nearly the same frequency under cloudy (103 times) and clear (115 times) conditions. There are, however, 147 instances of CALIOP AOD < 0.05 compared to only 19 instances of AERONET AOD < 0.05.

[51] Most cases of CALIOP AOD > AERONET AOD occur under cloudy conditions. In general, because CALIPSO does not detect optically thin layers in the column while AERONET integrates all layers, these cases are either symptomatic of cloud contamination or the use of incorrect lidar ratios in the AOD retrieval. The fact that most of these occur in cloudy sky conditions (36 points compared to seven points under clear sky conditions) suggests that cloud contamination is the primary cause. Of the poorly correlated coincidences, there are records at seven stations at which the CALIOP AOD under clear skies is greater than the AERONET AOD (Figure 14a). These are Bozeman, Canberra, CEILAP-RG, Issyk-Kul, Mauna Loa, Tamanrasset TMP, and Polar Environment Atmospheric Research Laboratory. The spatial and temporal offsets for these sites are shown in Table 5.

[52] These sites are located at or near the foothills of orographic formations or situated at mountain tops. At Mauna Loa, the AERONET site is located on northern slope of the Mauna Loa volcano about 3.4 km above the surface. In this case, at the point of closest coincidence the CALIPSO column extends to the surface on the opposite side of the mountain. As shown in Figure 15a, all of the Mauna Loa AERONET AOD < CALIPSO AOD, all the AERONET AOD are less than 0.05 consistent with free tropospheric measurements. The CALIPSO measurements extend into the planetary boundary layer at the foothills of Mauna Lao and are much larger than the AERONET measurement except for the lowest CALIOP AOD of 0.012.

[53] For Canberra the smallest CALIOP AOD is 0.034 (Figure 15b). There are significant differences between the instruments at the higher AOD. However, unlike Mauna Loa, the Canberra instrument is mounted on the roof of a two-story lab in an urban setting. The most likely cause of the discrepancies at Canberra is surrounding topography. Though the instrument is at an elevation of 600 m above sea level, it is surrounded by several hills and mountains which affect the measurements both by uneven surface heights and nonuniform aerosol structure due to orographic effects.

[54] Issyk-Kul (42°N,76°E) is surrounded by two giant mountainous chains: Kungey Ala-Too in the north, and Terskey Ala-Too in the south, which shield the site from continental pollution from large cities in the former Soviet republics, especially the large industrial center, Almaty, in neighboring Kazakhstan. On 4 September 2008 near 0800 UTC, CALIPSO observed a deep dust layer (about 3 km thick) just leeward of Kungey Ala-Too mountain range, which contributed to a relatively high AOD (0.42) retrieval. The AERONET AOD measured nearly contemporaneously about

Table 5. Cases of CALIOP AOD > AERONET AOD Among the Poorly Correlated Coincidences

Site Name	ΔT (min)	ΔX (km)	Elevation (m) amsl	CALIOP 532 nm AOD	AERONET 500 nm AOD
Bozeman	3.53	33.98	1530	0.226	0.0312
Canberra	0.22	33.76	600	0.3645	0.0832
CEILAP-RG	13.68	14.94	15	0.0338	0.0093
Issyk-Kul	1.24	29.05	1650	0.4207	0.0828
Mauna_Loa	6.50	17.20	3400	0.1563	0.0356
Tamanrasset_TMP	12.64	8.53	1377	2.4916	0.5281
Polar Environment Atmospheric Research Laboratory	5.0	25.2	615	0.8409	0.1077

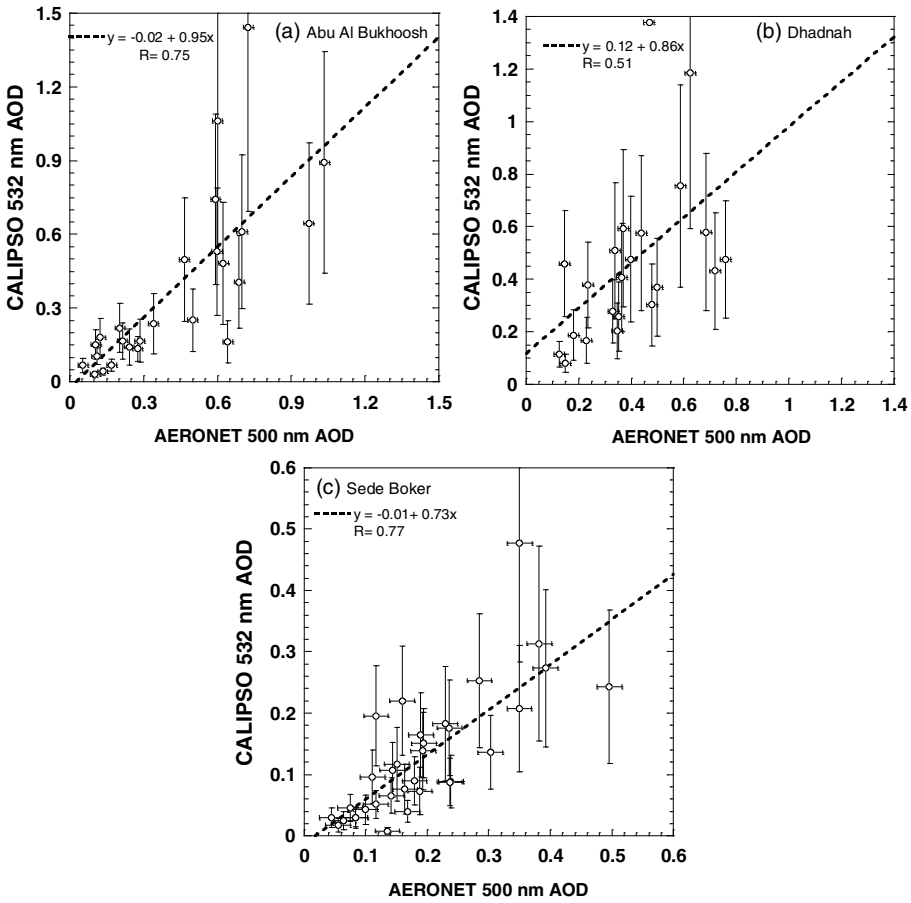

Figure 16. Comparison of CALIPSO and AERONET AOD at Abu Al Bukhoosh (25°N, 53°E), Dhadnah (25°N, 56°E), Sede Boker (30°N, 34°E) predominantly dust sites in desert regions in the Middle East.

30 km away was 0.08. It is therefore quite plausible that because of the complexity of the terrain surrounding the site, the two instruments record different air masses.

[55] Other sites in this category (Tamanrasset TMP and CEILAP-RG) have just one or two coincidences over the study period. Tamanrasset (22°N, 5°E) is in the highlands of the Algerian Sahara, near the source of Sahara dust. A spatial/temporal difference between CALIPSO and AERONET of 8.5 km/12.6 min in the vicinity of active dust sources may result in enough spatial inhomogeneity that the two instruments observed different dust concentrations. CEILAP-RG (51°S, 69°W) is a clean coastal site in Patagonia, Argentina, with AOD measurements below the uncertainty limits of both instruments.

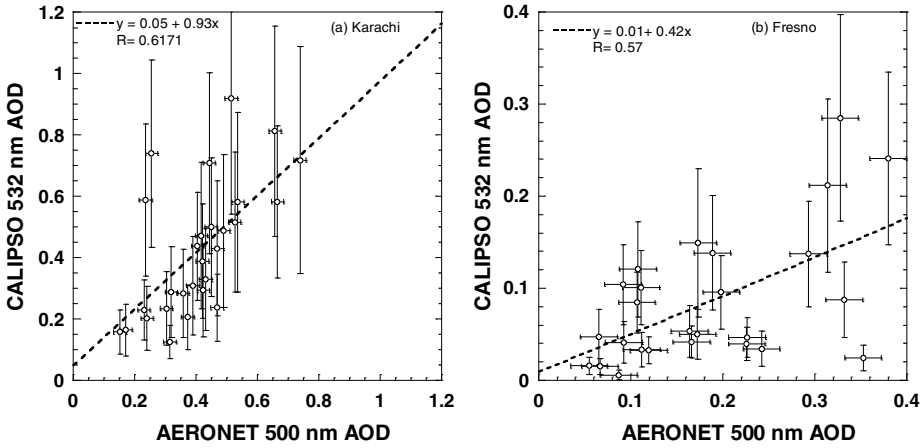

Figure 17. Comparison of CALIPSO and AERONET at (a) Karachi (24°N, 67°E), a large Asian urban center (population > 13 million) with different aerosol loadings, and (b) Fresno (36°N, 119°W), a relatively small U.S. city (population ~ 0.5 million).

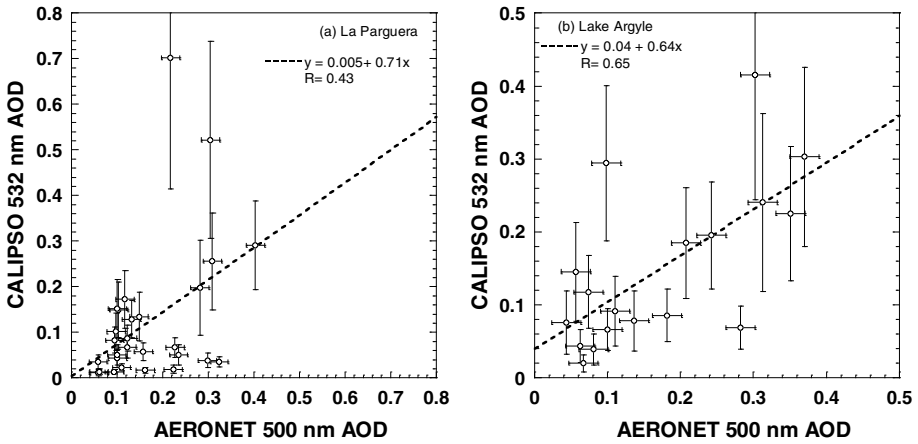

Figure 18. (a) The correlation for La Parguera (17°N, 67°W), a site in Puerto Rico that experiences dust, maritime and urban aerosol types and (b) Lake Argyle (16°S, 128°E), northern Australia, at which biomass burning smoke is prevalent.

[56] The Polar Environment Atmospheric Research Laboratory (80°N, 86°W) is part of AERONET Canada and is located in the Canadian Arctic facility near Eureka.

[57] At the closest point, the CALIPSO satellite ground track passes 25 km to the west of the station. For the small spatial and temporal difference between the two measurements, there is a large discrepancy between AODs. The terrain between the two instruments is mountainous and the surface is snow covered. It is possible the CALIOP AOD are affected by blowing snow more than the AERONET Sun photometer even if the latter is only 25 km away.

6. Correlations at Selected AERONET Stations

[58] In this section, we examine AOD correlation at sites associated with a predominant type of aerosol that have a reasonable number (~20) of coincidences. From Table 1, we have identified seven stations, discussed below, at which the local aerosol source types are dust (Abu Al Bukhoosh, Dhadnah, Sede Boker), urban pollution (Karachi, Fresno), smoke (Lake Argyle), and mixtures of urban, maritime and dust (La Parguera).

[59] The mean 500–1020 nm Ångström exponents (α) at Abu Al Bukhoosh, Dhadnah, and Sede Boker are 0.63, 0.88, and 1.0, respectively. These are all within the α-range (0–1.6) found for dust in Bahrain and Saudi Arabia by *Dubovik et al*. [2002b] and suggests that the predominant aerosol type at these sites is dust. The best correlation between CALIOP and AERONET AOD for this group is found at the Abu Al Bukhoosh station, located in the Arabian Sea, shown in Figure 16a. While, in general CALIOP AOD is somewhat lower at Dhadnah (Figure 16b) and Sede Boker (Figure 16c), there are a significant number of points where CALIOP AOD are larger than AERONET AOD implying that these differences are not necessarily dominated by a systemic bias, as one would expect from application of a low S_a for dust. For most, but not all of these points, dust is the dominant type and the S_a at 532 nm used for determining CALIOP dust optical depths is 40 sr [*Omar et al*., 2009].

[60] Figure 17 shows the correlation of CALIOP and AERONET AOD data for two urban areas with different aerosol loadings. Fresno is an urban site in central California's heavily polluted San Joaquin Valley [cf. *Ham and Kleeman*, 2011]. The mean α of 1.5 at Fresno is consistent with values at Greenbelt, MD and Crete-Paris ($1.2 < a < 2.3$), designated Urban-Industrial sites by *Dubovik et al*. [2002b]. Karachi is one of the world's largest cities, with AOD generally larger than 0.2. For Karachi the AOD correlations are generally better than at Fresno. For all but four of the Fresno coincidences, CALIPSO reported cloud free conditions. It is therefore unlikely that the poor correlations at Fresno are dominated by cloud contamination. The high frequency of low optical depth layers indicates that the daytime detection limitation of CALIOP is the primary cause of the discrepancy. The AERONET site at Karachi is located in a suburban area where local aerosol composition is dominated by mixtures of windblown dust and motor vehicles [*Mansha and Ghauri*, 2011]. Mean α for the Karachi records is 0.65 indicating such a mixture.

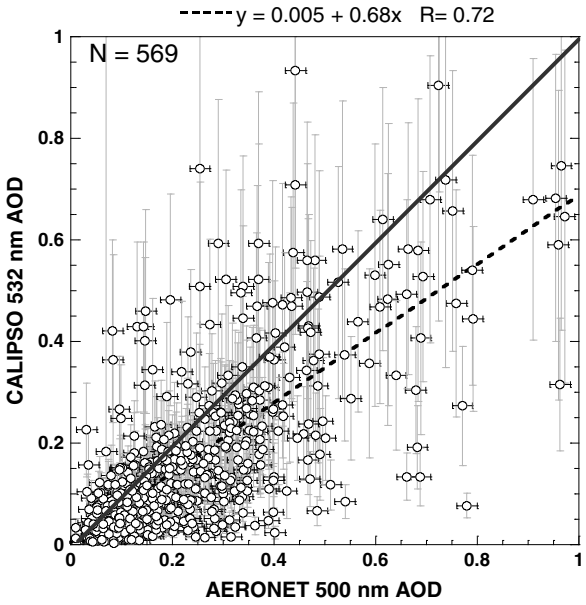

Figure 19. Cloud cleared data from 126 sites with Extinction Quality Flag ≤ 1, and AERONET AOD < 1.0. The dashed line is the regression line and the bold grey line is the one to one fit.

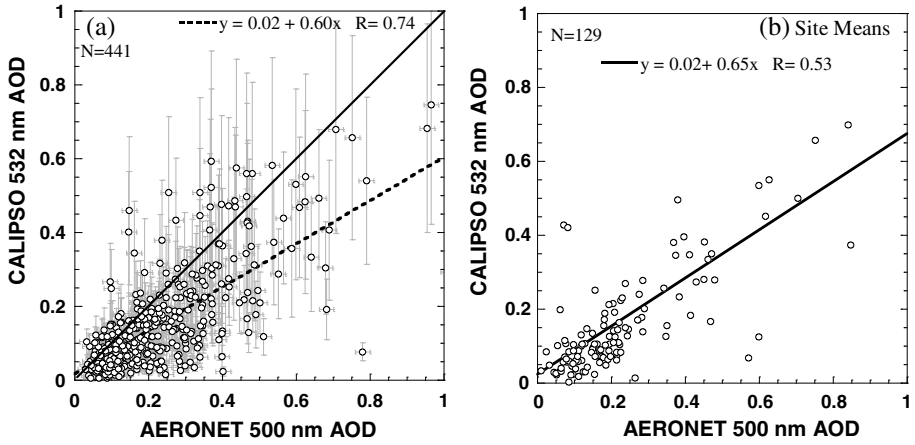

Figure 20. (a) Cloud cleared data from 112 AERONET sites with Extinction QC ≤ 1, the lowest CALIPSO layer < 1 km and RMSE < 0.2, and (b) cloud cleared mean AOD at individual AERONET sites, i.e., every data point is the averaged AOD from 2006 to 2010 at the site. In Figure 20a the bold line is the one to one relationship.

[61] La Parguera experiences marine, urban, and episodes of long range transport of dust [*Kalashnikova and Kahn*, 2008; *Reid et al*., 2003] from Sahara. The distribution of α at this site shows modes of small α (<0.5) and large α (>1.0) consistent with episodes of dust and urban pollution, respectively. Figure 18a shows the CALIOP-AERONET AOD correlation for this site. As for Fresno, the correlations are generally poor when the CALIOP AOD are less than 0.05. Mostly, these are sites where the CALIPSO algorithm detected clouds in the column. The Lake Argyle AERONET site is located in the Kimberly region of northern Australia near Lake Argyle, the largest interior body of water in the country. The site experiences biomass burning smoke aerosols about 84% of the time as well as episodic dust [*Qin and Mitchell*, 2009]. The mean α = 1.0, consistent with fine mode particles. The correlation in this case also degrades with smaller AOD (Figure 18b). The dust sites, heavily polluted urban sites, and in general sites with high AOD, have better correlations and smaller relative differences between the two instruments.

7. Effect of Data Screening on the Intercomparison

[62] In addition to cloud fraction, data points flagged for suspicious extinction retrievals, by virtue of an extinction QC flag greater than 1, may compromise these comparisons. Misclassification of (1) clouds as aerosols or (2) aerosols as clouds in CALIPSO CAD algorithms leads to errors of two kinds. In the case of (1), CALIOP AOD will be significantly higher than AERONET because of cloud contribution to the AOD. Case (2) leads to low CALIOP AOD corresponding to large AERONET AOD. This data set shows that Case (2) is more frequent.

[63] Figure 19 shows the regression between AERONET AOD and CALIOP AOD when screening criteria are applied that exclude high AERONET AOD (>1.0), and points corresponding with cloudy columns using the CALIPSO cloud mask and Extinction QC values greater than 1. The exclusion of large AERONET AOD is applied as a first order estimate to ensure that the column is not cloud contaminated. The mean relative difference between the two measurements is 25% of the AERONET AOD and the median relative difference is 36% of the AERONET AOD. The standard deviation of the difference is 64% of the AERONET AOD.

[64] In Figure 20, we have applied screening criteria based on (1) ExtQC to ensure only records with high confidence retrievals, (2) the location of the base of aerosol layer (> 1 km), to exclude data with layer bases of the lowest aerosol layer that do not extend into the boundary layer, (3) an RMSE threshold to exclude data with RMSE greater than 0.2 ensuring scene homogeneity, and (4) clear skies by CALIPSO cloud mask. Using these screening criteria, the median relative difference between the two measurements is 30% of the AERONET AOD and the mean relative difference is 35% with a standard deviation of 31%.

[65] These screening filters additionally improve the correlation coefficients of the regression by a significant margin from 0.42 (Figure 6b, all sky) and 0.57 (Figure 6a, clear sky) to 0.74 in Figure 20a. The site-averaged cloud cleared AOD is shown in Figure 20b. While the regression slope of the site-averaged AOD is slightly better than that in Figure 20a, the regression coefficient is worse because of the disproportionate effect of stations with a few outlying records.

8. Conclusion

[66] Direct validation of space based lidar measurements are complicated by the lack of similar ground based lidars except for a few regions. Comparisons with passive measurements are precarious because the footprint of the lidar is an order of magnitude smaller than the smallest passive satellite resolution. The site by site comparisons with AERONET Sun photometers provide the next best opportunity albeit for the comparison of a direct quantity (AERONET AOD) to a retrieved quantity (CALIOP AOD).We have compared the AOD of CALIOP (532 nm) and AERONET (500 nm) over a 4 year period (2006–2010) using CALIPSO quality assurance flags for retrieval uncertainty, cloudiness, aerosol layer location, and aerosol homogeneity to screen the data. In all we found 1081 coincident points at 92 land and 57 ocean/coastal

AERONET sites. In 45% of the coincident instances CALIOP and AERONET do not agree on the cloudiness of the scenes. When cloud cleared and extinction quality controlled CALIOP data is compared with AERONET data with AOD less than 1.0, the mean and median relative difference between the two measurements is 25% and 36% of AERONET AOD, respectively. In general, CALIOP AOD is smaller than AERONET AOD. This is the case whether we compare CALIOP AOD with AERONET land or ocean/coastal sites and may be because CALIOP does not detect some tenuous layers at daytime because of low SNR. While the individual AOD of these missed layers is small, the integrated AOD is substantial.

[67] We find that CALIOP detects up to 20% more features at night, than during the day globally and nearly 10% more features at night in environments where diurnal differences are expected to be small (e.g., remote marine environments). The recommendations for a high fidelity daytime AOD comparison between CALIOP or similar space-based backscatter lidar and AERONET or similar surface-based Sun photometer, emanating out of this study are therefore, as follows: (1) cloud cleared data using the lidar cloud mask, (2) high confidence retrievals, e.g., correct and unchanged S_a, (3) homogeneous scenes determined by examining adjacent columns, and (4) fairly level surface around the AERONET station to ensure lidar column and Sun photometer column are of the same depth. Lunar or star photometers in place of Sun photometers following the same protocols to measure nighttime AOD would provide answers to questions raised in this paper about the extent to which low SNR might contribute to CALIOP's lower AOD. Upcoming refinements to CALIOP algorithms will yield improved estimates of AOD and, data possibly contaminated by cirrus clouds may be removed in a later version of AERONET products using an improved cloud screening algorithm. Both of these should lead to improvements in the correlations between the two measurements.

[68] **Acknowledgments.** We thank the AERONET Principal Investigators and their staff for establishing and maintaining the AERONET at the 149 sites used in this investigation, and three reviewers for providing detailed substantive suggestions for improving the original manuscript.

References

Anderson, T. L., A. R. J. Charlson, D. M. Winker, J. A. Ogren, and K. Holmen (2003), Mesoscale Variations Of Tropospheric Aerosols, *J. Atmos. Sci.*, *60*, 119–136.

Bloom, S. A., et al. (2005), Documentation and validation of the Goddard Earth Observing System (GEOS) data assimilation system version 4, NASA Tech. Rep. NASA/TM-2005-104606, Vol. 26, 187 pp.

Bréon, F.-M., A. Vermeulen, and J. Descloitres (2011), An evaluation of satellite aerosol products against sunphotometer measurements, *Rem. Sens. Environ.*, *115*(12), 3102–3111.

Campbell, J. R., K. Sassen, and E. J. Welton (2008), Elevated Cloud and Aerosol Layer Retrievals from Micropulse Lidar Signal Profiles, *J. Atmos. Ocean Tech.*, *25*(5), 685–700.

Campbell, J. R., et al. (2012), Evaluating nighttime CALIOP 0.532 μm aerosol optical depth and extinction coefficient retrievals, *Atmos. Meas. Tech. Discuss.*, *5*(2), 2747–2794.

Chew, B. N., J. R. Campbell, J. S. Reid, D. M. Giles, E. J. Welton, S. V. Salinas, and S. C. Liew (2011), Tropical cirrus cloud contamination in sun photometer data, *Atmos. Environ.*, *45*(37), 6724–6731.

Chu, D. A., Y. J. Kaufman, C. Ichoku, L. A. Remer, D. Tanré, and B. N. Holben (2002), Validation of MODIS aerosol optical depth retrieval over land, *Geophys. Res. Letts.*, *29*(12), doi:10.1029/2001GL013205.

de Meij, A., S. Wagner, C. Cuvelier, F. Dentener, N. Gobron, P. Thunis, and M. Schaap (2007), Model evaluation and scale issues in chemical and optical aerosol properties over the greater Milan area (Italy), for June 2001, *Atmos. Res.*, *85*(2), 243–267.

Derimian, Y., A. Karnieli, Y. J. Kaufman, M. O. Andreae, T. W. Andreae, O. Dubovik, W. Maenhaut, and I. Koren (2008), The role of iron and black carbon in aerosol light absorption, *Atmos. Chem. Phys.*, *8*(13), 3623–3637.

Dubovik, O., and M. D. King (2000), A flexible inversion algorithm for retrieval of aerosol optical properties from Sun and sky radiance measurements, *J. Geophys. Res.*, *105*, 9791–9806.

Dubovik, O., B. N. Holben, T. Lapyonok, A. Sinyuk, M. I. Mischenko, P. Yang, and I. Slutsker (2002a), Non-spherical aerosol retrieval method employing light scattering by spheroids, *Geophys. Res. Letts.*, *29*(10).

Dubovik, O., B. N. Holben, T. F. Eck, A. Smirnov, Y. J. Kaufman, M. D. King, D. Tanre, and I. Slutsker (2002b), Variability of absorption and optical properties of key aerosol types observed in worldwide locations, *J. Atmos. Sci.*, *59*, 590–608.

Eck, T. F., B. N. Holben, J. S. Reid, O. Dubovik, A. Smirnov, N. T. O'Neill, I. Slutsker, and S. Kinne (1999), Wavelength dependence of the optical depth of biomass burning, urban, and desert dust aerosols, *J. Geophys. Res.*, *104*(D24), 31,333–31,349.

Eck, T. F., et al. (2010), Climatological aspects of the optical properties of fine/coarse mode aerosol mixtures, *J. Geophys. Res.*, *115*.

Giles, D. M., et al. (2011), Aerosol properties over the Indo-Gangetic Plain: A mesoscale perspective from the TIGERZ experiment, *J. Geophys. Res.*, *116*.

Goloub, P., D. Tanre, J. L. Deuze, M. Herman, A. Marchand, and F. M. Breon (1999), Validation of the first algorithm applied for deriving the aerosol properties over the ocean using the POLDER ADEOS measurements, *IEEE Trans. Geosci. Rem. Sens.*, *37*(3), 1586–1596.

Ham, W. A., and M. J. Kleeman (2011), Size-resolved source apportionment of carbonaceous particulate matter in urban and rural sites in central California, *Atmos. Environ.*, *45*(24), 3988–3995.

Hatakeyama, S., K. Izumi, and H. Akimoto (1985), Yield of SO2 and formation of aerosol in the photo-oxidation of DMS under atmospheric conditions, *Atmos. Environ.*, *19*(1), 135–141.

Holben, B. N., T. F. Eck, I. Slutsker, A. Smirnov, A. Sinyuk, J. Schafer, D. Giles, and O. Dubovik (2006), AERONET's version 2.0 quality assurance criteria, in *Proc. SPIE Int. Soc. Opt. Eng.*, edited by S.-C. Tsay et al., pp. 1–14.

Holben, B. N., et al. (1998), AERONET - A federated instrument network and data archive for aerosol characterization, *Rem. Sens. Env.*, *66*, 1–16.

Hu, Y., et al. (2009), CALIPSO/CALIOP Cloud Phase Discrimination Algorithm, *J. Atmos. Oceanic Technol.*, *26*(11), 2293–2309.

Huang, J. F., N. C. Hsu, S. C. Tsay, M. J. Jeong, B. N. Holben, T. A. Berkoff, and E. J. Welton (2011), Susceptibility of aerosol optical thickness retrievals to thin cirrus contamination during the BASE-ASIA campaign, *J. Geophys. Res.*, *116*.

Kacenelenbogen, M., M. A. Vaughan, J. Redemann, R. M. Hoff, R. R. Rogers, R. A. Ferrare, P. B. Russell, C. A. Hostetler, J. W. Hair, and B. N. Holben (2011), An accuracy assessment of the CALIOP/CALIPSO version 2/ version 3 daytime aerosol extinction product based on a detailed multi-sensor, multi-platform case study, *Atmos. Chem. Phys.* , *11*(8), 3981–4000.

Kahn, R. A., B. J. Gaitley, J. V. Martonchik, D. J. Diner, K. A. Crean, and B. Holben (2005), Multiangle Imaging Spectroradiometer (MISR) global aerosol optical depth validation based on 2 years of coincident Aerosol Robotic Network (AERONET) observations, *J. Geophys. Res.*, *110*(D10), doi:10.1029/2004JD004706.

Kahn, R. A., B. J. Gaitley, M. J. Garay, D. J. Diner, T. F. Eck, A. Smirnov, and B. N. Holben (2010), Multiangle Imaging SpectroRadiometer global aerosol product assessment by comparison with the Aerosol Robotic Network, *J. Geophys. Res.*, *115*(D23), D23209.

Kalashnikova, O. V., and R. A. Kahn (2008), Mineral dust plume evolution over the Atlantic from MISR and MODIS aerosol retrievalsy, *J. Geophys. Res.*, *113*.

Kaufman, Y. J., G. P. Gobbi, and I. Koren (2006), Aerosol climatology using a tunable spectral variability cloud screening of AERONET data, *Geophys. Res. Lett.*, *33*(7), L07817.

Kaufman, Y. J., et al. (2005), A critical examination of the residual cloud contamination and diurnal sampling effects on MODIS estimates of aerosol over ocean, *IEEE Trans. Geosci. Rem. Sens.*, *43*(12), 2886–2897.

Kittaka, C., D. M. Winker, M. A. Vaughan, A. Omar, and L. A. Remer (2011), Intercomparison of column aerosol optical depths from CALIPSO and MODIS-Aqua, *Atmos. Meas. Tech.*, *4*(2), 131–141.

Levy, R. C., L. A. Remer, R. G. Kleidman, S. Mattoo, C. Ichoku, R. Kahn, and T. F. Eck (2010), Global evaluation of the Collection 5 MODIS dark-target aerosol products over land, *Atmos. Chem. Phys.*, *10*(21), 10,399–10,420.

Liu, Z. Y., D. Winker, A. Omar, M. Vaughan, C. Trepte, Y. Hu, K. Powell, W. B. Sun, and B. Lin (2011), Effective lidar ratios of dense dust layers over North Africa derived from the CALIOP measurements, *J. Quant. Spectroscopy & Radiative Transfer*, *112*(2), 204–213.

Liu, Z. Y., M. Vaughan, D. Winker, C. Kittaka, B. Getzewich, R. Kuehn, A. Omar, K. Powell, C. Trepte, and C. Hostetler (2009), The CALIPSO Lidar Cloud and Aerosol Discrimination: Version 2 Algorithm and Initial Assessment of Performance, *J. Atmos. Oceanic Technol.*, *26*(7), 1198–1213.

Mansha, M., and B. Ghauri (2011), Assessment of fine particulate matter (PM2.5) in metropolitan Karachi through satellite and ground–based measurements, *J. Appl. Rem. Sens.*, *5*(1), 053546–053546.

McPherson, C. J., J. A. Reagan, J. Schafer, D. Giles, R. Ferrare, J. Hair, and C. Hostetler (2010), AERONET, airborne HSRL, and CALIPSO aerosol retrievals compared and combined: A case study, *J. Geophys. Res.*, *115*, D00H21.

Nwofor, O. K., T. Chidiezie Chineke, and R. T. Pinker (2007), Seasonal characteristics of spectral aerosol optical properties at a sub-Saharan site, *Atmospheric Research*, *85*(1), 38–51.

Omar, A., et al. (2009), The CALIPSO automated aerosol classification and lidar ratio selection algorithm, *J. Atmos. Oceanic Technol.*, *26*(10), 1994–2014.

Powell, K. A., et al. (2009), CALIPSO Lidar Calibration Algorithms. Part I: Nighttime 532-nm Parallel Channel and 532-nm Perpendicular Channel, *J. Atmos. Ocean. Tech.*, *26*(10), 2015–2033.

Qin, Y., and R. M. Mitchell (2009), Characterisation of episodic aerosol types over the Australian continent, *Atmos. Chem. Phys.*, *9*(6), 1943–1956.

Redemann, J., M. A. Vaughan, Q. Zhang, Y. Shinozuka, P. B. Russell, J. M. Livingston, M. Kacenelenbogen, and L. A. Remer (2012), The comparison of MODIS-Aqua (C5) and CALIOP (V2 & V3) aerosol optical depth, *Atmos. Chem. Phys.*, *12*(6), 3025–3043.

Reid, J. S., et al. (2003), Analysis of measurements of Saharan dust by airborne and ground-based remote sensing methods during the Puerto Rico Dust Experiment (PRIDE), *J. Geophys. Res.*, *108*(D19), doi:10.1029/2002JD002493.

Remer, L. A., et al. (2002), Validation of MODIS aerosol retrieval over ocean, *Geophys. Res. Letts.*, *29*(12), doi:10.1029/2001GL013204.

Remer, L. A., et al. (2005), The MODIS aerosol algorithm, products, and validation, *J. Atmos. Sci.*, *62*, 947–973.

Seinfeld, J. H., and S. N. Pandis (1998), Atmospheric chemistry and physics: from air pollution to climate change, xxvii, 1326 pp., Wiley, New York; Chichester.

Sidebottom, H. W., C. C. Badcock, G. E. Jackson, J. G. Calvert, G. W. Reinhardt, and E. K. Damon (1972), Photooxidation of sulfur dioxide, *Environ. Sci. Technol.*, *6*(1), 72–79.

Smirnov, A., B. N. Holben, T. F. Eck, O. Dubovik, and I. Slutsker (2000), Cloud-screening and quality control algorithms for the AERONET database, *Rem. Sens. Env.*, *73*, 337–349.

Smirnov, A., B. N. Holben, T. F. Eck, O. Dubovik, and I. Slutsker (2003), Effect of wind speed on columnar aerosol optical properties at Midway Island, *J. Geophys. Res.*, *108*(D24), doi:10.1029/2003JD003879.

Vaughan, M. A., K. A. Powell, R. E. Kuehn, S. A. Young, D. M. Winker, C. A. Hostetler, W. H. Hunt, Z. Y. Liu, M. J. McGill, and B. J. Getzewich (2009), Fully Automated Detection of Cloud and Aerosol Layers in the CALIPSO Lidar Measurements, *J. Atmos. Oceanic Technol.*, *26*(10), 2034–2050.

Vernier, J. P., et al. (2011), Major influence of tropical volcanic eruptions on the stratospheric aerosol layer during the last decade, *Geophys. Res. Lett.*, *38*(12), L12807.

Winker, D., W. H. Hunt, and M. J. McGill (2007), *Initial performance assessment of CALIOP*, Geophys. Res. Letts., *34*(19).

Winker, D., M. A. Vaughan, A. Omar, Y. X. Hu, K. A. Powell, Z. Y. Liu, W. H. Hunt, and S. A. Young (2009), Overview of the CALIPSO Mission and CALIOP Data Processing Algorithms, *J. Atmos. Oceanic Technol.*, *26*(11), 2310–2323.

Young, S. A. (1995), Analysis of lidar backscatter profiles in optically thin clouds, *Appl. Opt.*, *34*(30), 7019–7031.

Young, S. A., and M. A. Vaughan (2009), The Retrieval of Profiles of Particulate Extinction from Cloud-Aerosol Lidar Infrared Pathfinder Satellite Observations (CALIPSO) Data: Algorithm Description, *J. Atmos. Oceanic Technol.*, *26*(6), 1105–1119.

Young, S. A., M. A. Vaughan, R. E. Kuehn, and D. M. Winker (2012), The Retrieval of Profiles of Particulate Extinction from Cloud-Aerosol Lidar Infrared Pathfinder Satellite Observations (CALIPSO) Data: Uncertainty and Error Sensitivity Analyses, *J. Atmos. Ocean Tech.*, *In Press*.

Zhang, J., and J. S. Reid (2006), MODIS aerosol product analysis for data assimilation: Assessment of over-ocean level 2 aerosol optical thickness retrievals, *J. Geophys. Res.*, *111*(D22), D22207.